Marine Micropaleontology 136 (2017) 51–65

Contents lists available at ScienceDirect

Marine Micropaleontology

journal homepage: www.elsevier.com/locate/marmicro

Neogene dinoflagellate cysts and acritarchs from the high northern latitudes and their relation to sea surface temperature

Michael Schreck[a,b,*], Seung-Il Nam[b], Caroline Clotten[c], Kirsten Fahl[d], Stijn De Schepper[c], Matthias Forwick[a], Jens Matthiessen[d]

[a] *Department of Geosciences, UiT The Arctic University of Norway in Tromsø, P.O. Box 6050, Langnes, 9037 Tromsø, Norway*
[b] *Division of Polar Environment, Korea Polar Research Institute, 26 Songdomirae-ro, Yeonsu-gu, 21990 Incheon, Republic of Korea*
[c] *Uni Research Climate, Bjerknes Centre for Climate Research, Jahnebakken 5, 5007 Bergen, Norway*
[d] *Alfred Wegener Institute Helmholtz Centre for Polar and Marine Research, Am Alten Hafen 26, 27568 Bremerhaven, Germany*

ARTICLE INFO

Keywords:
Iceland Sea
Neogene
Dinoflagellate cyst
Acritarch
Alkenones
Paleotemperatures

ABSTRACT

Organic-walled dinoflagellate cysts and acritarchs are a vital tool for reconstructing past environmental change, in particular in the Neogene of the high northern latitudes where marine deposits are virtually barren of traditionally used calcareous microfossils. Yet only little is known about the paleoenvironmental value of fossil assemblages that do not have modern analogues, so that reconstructions remain qualitative. Thus, extracting their paleoecological signals still poses a major challenge, in particular on pre-Quaternary timescales. Here we unravel the relationship between species relative abundance and sea surface temperature for extinct dinoflagellate cyst and acritarch taxa from the Neogene of the Iceland Sea using palynological assemblages and organic geochemical (alkenone) data generated from the same set of samples. The reconstructed temperatures for the Miocene to Pliocene sequence of Ocean Drilling Program Site 907 range from 3 to 26 °C and our database consists of 68 dinoflagellate cyst and acritarch samples calibrated to alkenone data. The temperature range of five extant species co-occurring in the fossil assemblage agrees well with their present-day distribution providing confidence to inferred temperature ranges for extinct taxa. The 14 extinct dinoflagellate cyst and acritarch species clearly exhibit a temperature dependency in their occurrence throughout the analysed section. The dinoflagellate cyst species *Batiacasphaera hirsuta*, *Labyrinthodinium truncatum*, *Cerebrocysta irregulare*, *Cordosphaeridium minimum*, *Impagidinium elongatum* and *Operculodinium centrocarpum* s.s., and the acritarch *Lavradosphaera elongatum*, which are confined to the Miocene, have highest relative abundances and restricted temperature ranges at the warm end of the reconstructed temperature spectrum. The latter five species disappear when Iceland Sea surface temperatures permanently drop below 20 °C, thus indicating a distinct threshold on their occurrence. In contrast, species occurring in both the Miocene and Pliocene interval (*Batiacasphaera micropapillata*, *Habibacysta tectata*, *Reticulatosphaera actinocoronata*, *Cymatiosphaera*? *invaginata*) show a broader temperature range and a tolerance towards cooler conditions. *Operculodinium*? *eirikianum* may have a lower limit on its occurrence at around 10 °C.

The calibration of species relative abundance versus reconstructed sea surface temperature provides a quantitative assessment of temperature ranges for extinct Miocene to Pliocene species indicating that temperature is a decisive ecological factor for regional extinctions that may explain the frequently observed asynchronous highest occurrences across different ocean basins. It demonstrates that qualitative assessments of ecological preferences solely based on (paleo) biogeographic distribution should be treated with caution. In addition to enhancing knowledge on marine palynomorph paleoecology, this study ultimately improves the application of palynomorphs for paleoenvironmental reconstructions in the Neogene of the Arctic and subarctic seas, a region essential for understanding past global climate.

1. Introduction

Due to the nearly complete absence of biosiliceous and calcareous microfossils in Neogene deposits at high northern latitudes, organic-walled marine palynomorphs (dinoflagellate cysts and acritarchs) are important proxies for the establishment of a regional biostratigraphy and paleoenvironmental reconstructions in the Arctic and sub-arctic realm (e.g. Schreck et al., 2012, 2013; De Schepper et al., 2015, 2017).

---

[*] Corresponding author at: Department of Geosciences, UiT The Arctic University of Norway in Tromsø, P.O. Box 6050, Langnes, 9037 Tromsø, Norway.
E-mail address: Michael.Schreck@uit.no (M. Schreck).

http://dx.doi.org/10.1016/j.marmicro.2017.09.003
Received 26 August 2016; Received in revised form 18 August 2017; Accepted 11 September 2017

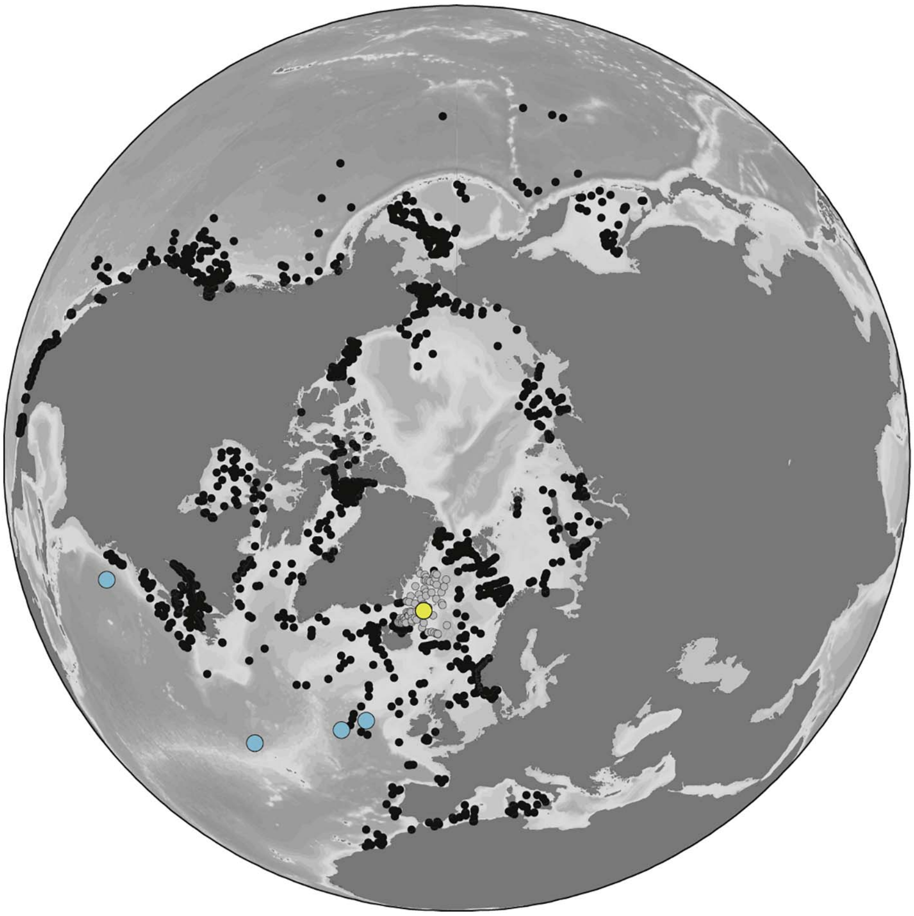

Fig. 1. Location of the study site ODP Site 907 (yellow dot) and the sites of the n = 1492 present-day Northern Hemisphere reference database of de Vernal et al., 2013 (black and grey dots) and the n = 101 Nordic Seas subset (grey dots only). Blue dots represent the Pliocene to Pleistocene North Atlantic sites of the n = 204 paleo-database (De Schepper et al., 2011). (For interpretation of the references to colour in this figure legend, the reader is referred to the web version of this article.)

They have been proven particularly useful in upper Quaternary deposits where assemblages are comparable to modern assemblages (de Vernal et al., 2005). The distribution of modern dinoflagellate cysts (dinocysts) at high northern latitudes was first studied on locally restricted data sets, which were subsequently expanded and combined within a Northern Hemisphere reference database that currently comprises 1492 sites (Fig. 1; e.g. de Vernal et al., 2013 and references therein). The present-day n = 1492 database documents the relationship between species relative abundance and observed surface water parameters, which control assemblage composition. This extensive reference dataset has been widely used to quantitatively reconstruct sea surface temperature, salinity, productivity and sea ice cover in upper Quaternary sediments (e.g. Radi and de Vernal, 2008; de Vernal et al., 2001, 2013; Van Nieuwenhove et al., 2016) using transfer functions (e.g. Modern Analogue Technique, Guiot and de Vernal, 2007).

Reconstructions of Neogene high latitude paleoceanographic and paleoclimatic variability relies heavily on marine palynomorphs, which are often the only microfossil group with a continuous record in pre-Quaternary sediments in this region. However, when going further back in the Neogene, palynomorph assemblages are increasingly dominated by extinct species of which the ecological affinities are poorly constrained. Therefore, it is of crucial importance to unravel the (paleo)ecology of these Neogene marine palynomorphs in order to improve their application for paleoceanographic studies in a region essential for understanding the Cenozoic transition from greenhouse to icehouse climates.

In the past decades, significant progress has been made in deciphering the paleoecology of extinct species using statistical analyses (e.g. Versteegh and Zonneveld, 1994), the definition of paleoenvironmental indices (Edwards et al., 1991; Versteegh, 1994), and analysis of the biogeographic distribution (Head, 1997; Masure and Vrielynck, 2009; Schreck and Matthiessen, 2013). The derived information, however, solely remains qualitative (e.g. warm/cold, oceanic/neritic). Recently, geochemical proxies for sea surface conditions have been employed to directly assess the paleoecology of extinct species (De Schepper et al., 2011; Hennissen et al., 2017). De Schepper et al. (2011) correlated the relative abundance of extant species to a sea surface temperature (SST) proxy derived from the same sample and then compared to the species' modern temperature distribution using the n = 1171 dataset (the n = 1492 precursor) of Radi and de Vernal (2008) and a subset thereof. The subset was restricted to 518 samples located mainly in the North Atlantic Ocean between 75°W and 15°E, and north of 25°N, with samples from the Mediterranean and northern part of Baffin Bay being omitted (De Schepper et al., 2011). Based on a dataset containing 204 samples from four drilling sites across the Plio-Pleistocene North Atlantic (Fig. 1), the authors demonstrated a strong correlation between reconstructed and present-day SST ranges of extant species. Because modern species occurring in fossil assemblages have a comparable temperature distribution as today, De Schepper et al. (2011) argued that SST ranges of extinct species could be determined with confidence. Using this approach, they documented past temperature ranges of 16 extinct dinocyst species from the Plio-Pleistocene North Atlantic in their n = 204 paleo-database.

Based on this approach, we establish a quantitative relationship between high latitude marine palynomorph species and alkenone-based SST for the Miocene to Pliocene interval of Ocean Drilling Program (ODP) Hole 907A in the Iceland Sea. Both palynological assemblage and organic geochemical data are extracted from the same sample to ensure one-to-one comparability. Therefore, this study provides independently derived temperature affinities of extinct species, and refines previous ecological interpretations that were solely based on biogeographic

Epoch	Age	Chron	Magnetostratigraphy 907A (Channell et al., 1999)	Lithological units	Depth mbsf	Core	Section	Interval in cm	Calibrated ages	Sea surface temperature (°C)	Dinoflagellate cysts																	Acritarchs					
											Habibacysta tectata	*Spiniferites elongatus* s.l.	*Nematosphaeropsis labyrinthus*	*Batiacasphaera micropapillata*	*Impagidinium pallidum*	*Operculodinium tegillatum*	*Operculodinium? eirikianum*	*Reticulatosphaera actinocoronata*	*Ataxiodinium choane*	*Lingulodinium machaerophorum*	*Batiacasphaera hirsuta*	*Labyrinthodinium truncatum*	*Impagidinium elongatum*	*Cerebrocysta irregulare*	*Cordosphaeridium minimum*	*Operculodinium centrocarpum* s.s.	Total in-situ dinocyst counts	*Cymatiosphaera ? invaginata*	*Lavradosphaera crista*	*Decahedrella martinheadii*	*Lavradosphaera elongata*	Total in-situ acritarch counts	Total in-situ palynomorph counts
Pliocene	Piacenzian	Gauss		II	49.10	6	3	82–84	2.59																		4						4
					*50.83	6	4	103–105	2.68	12.37	18		3														205	4061	37			4164	4369
			C2An.1n		51.10	6	4	130–132	2.69																		3	1				1	4
					53.00	6	6	16.5–18.5	2.78		3	1															7	2				2	9
					55.10	7	1	30–32	2.89				5														7	4				4	11
				IIIA	56.60	7	2	31–33	2.97																		2						2
			C2An.1r		58.00	7	3	17–19	3.04	9.09	3																2	1				2	4
			C2An.2n		60.30	7	4	102–104	3.16	9.97																	2						2
			C2An.3n		62.20	7	5	137.5–139.5	3.27																		9						9
					63.20	7	6	87–89	3.34																		403						403
					64.20	7	7	41–43	3.42	18.09				4		(1)											407					1	408
					*64.42	8	1	12–14	3.43	7.08																	249						249
					65.20	8	1	90–92	3.48					1													2					1	3
					66.20	8	2	40–42	3.55	7.77																	0						
	Zanclean	Gilbert	C2Ar		67.20	8	2	140–142	3.66	7.86			3	3	12												196						196
					68.20	8	3	90–92	3.82	6.87			1														10						10
					69.20	8	4	43–45	3.98	10.36																	0						
					70.20	8	4	140-142	4.14	9.84																	0						
			C3		71.20	8	5	90-92	4.26	9.92		3	73	2	4												137	1				1	138
					72.10	8	6	32-34	4.34	9.55		1	20		4												53	1				2	55
					73.20	8	6	140-142	4.45	13.43				2	10	4	3	1									367					5	372
					74.20	9	1	40-42	4.55	12.10		1	137	63	7	2	2	5									414	130	52			290	704
					75.20	9	1	140-142	4.64	7.04	*	13	30		1	1											362	39	25			114	476
					*75.62	9	2	32-34	4.68	13.35		43	71	147	3	3		1									451	109	3			248	699
					76.20	9	2	90-92	4.74			37	41	167	2	19	*	1	*								355	255	17			351	706
					*76.22	9	2	92-94	4.74	13.36		145	26	14		5											363	205	3			319	682
					77.20	9	3	41-43	4.84	11.22	*	196	17	16		20	5	6			(2)						393	186	3			392	785
					*77.27	9	3	47-49	4.85	12.93		37	57	209	2	1	1										346	363				437	783
					*77.97	9	3	117-119	4.91	13.38				5	1												241	32				139	380
					78.20	9	3	140-142	4.94	8.92	1	5		9		12	*	2									379	24	2			35	414
					79.20	9	4	93-95	5.04	12.45		2	1	11	8		1										28					80	108
					80.20	9	5	40-42	5.13	10.15	4		64	6		2		1									89	1				199	288
					81.20	9	5	140-142	5.23	10.08	2		99				1										134	4				4	138
					82.20	9	6	90-92	5.32				140		1				2								173						173
Late Miocene	Messinian				83.20	9	7	40-42	5.42	11.47			284						1		(*)						351	2				49	400
					84.20	10	1	88-90	5.52		1		18		1			8	3								72	60				67	139
					85.20	10	2	40-42	5.62	8.26			285				1										459	3				3	462
					86.20	10	2	140-142	5.71				145	5			2										377	3				3	380
					87.20	10	3	90-92	5.81		*		179	4				1	10								392	15				16	408
					88.00	10	4	17.5-19.5	5.88	11.14	1		1					1	3								33						33
					89.20	10	4	140-142	6.00	12.81	1		13														30						30
		C3A	C3An.1n		90.40	10	5	110-112	6.10	14.73			28		2		1										51					1	52
					91.70	10	6	87-89	6.21	8.40	16		195	2	5				7								363	30				32	395
			C3An.1r		92.30	10	7	1-3	6.26	9.06	6				1												35	1		2		5	40
					92.90	11	1	11-13	6.37	5.10																	0						
			C3An.2n	IIIB	93.50	11	1	73-75	6.46	3.38	2		3							*							28			363		364	392
					94.40	11	2	11-13	6.54	11.18	17		15		1											(*)	64			355		356	420
					95.50	11	2	121-123	6.65	11.01			29	24					24								227	*		185		189	416
			C3Ar		96.40	11	3	60-62	6.73	13.62	1			22	2		1		2								251	3		120		128	379
					97.00	11	3	117.5-119.5	6.85		5		339		1			1	*	*							363	1		12		18	381
					97.40	11	4	12-14	6.95	12.78		1	10			1											13	2				2	15
					98.00	11	4	69.5-71.5	7.07	11.68	13		70	171	13		5	21	54		(1)						401	1		6		61	462
		C3B			98.50	11	4	121-123	7.18	15.12	17		23	71	1		3	87	30								365			31		66	431
	Tortonian				99.00	11	5	18-20	7.28	15.51	13		242	1				2	7								318			60		68	386
					99.60	11	5	77-79	7.40	18.32			1														1						1
					100.00	11	5	122-124	7.50	16.71			2														3	1				1	4
		C4			100.50	11	6	20-22	7.60	17.42								1									1						1
					101.10	11	6	77-79	7.72																		0						
					101.40	11	6	111-113	7.79																		0					1	1
					101.90	11	7	7-9	7.89	17.85																	0	1				1	1
					102.50	12	1	20-22	8.02	13.53			1														1						1
					103.10	12	1	77-79	8.14	17.67			12														14	1		1		2	16
					103.60	12	1	127-129	8.25	17.06	2		22	13	3			1		2							75			7		7	82
					104.00	12	2	22-24	8.34	14.74	11		37	216	12		5	9	8	1							360			21		38	398
			condensed section		104.50	12	2	68-70	8.44		10		51	129	16		2	15	4	1	3	7					365	1		7		48	413
					105.10	12	2	127-129	8.56	17.50			10	41													397			5		9	406
					105.50	12	3	20-22	8.66		1		4	310	3	*		*				*					355			8		14	369
		C4A			106.10	12	3	77-79	8.78		43		149	180						*	2	3					392			5		11	403
					106.60	12	3	127-129	8.88	15.22	24		75	155	4	1	1			*		1					288			97		100	388
					107.00	12	4	18-20	8.97	18.67	15		52	143	1		1	2		*	1	27					316			46		67	383
					107.60	12	4	77-79	9.09	16.68	8		47	115	2		*	4				18					239	2		135		142	381
					107.90	12	4	111.5-113.5	9.17		6		25	116	2			3				10					289	1		101		106	395
					108.50	12	5	19-21	9.29	17.60	6		85	69			*	2				18					291	2		72		77	368
					109.10	12	5	82.5-84.5	9.42	17.96	4		218	15				4				33					336	2		39		55	391
					109.50	12	5	123-125	9.51	21.05	12		93	27	3		5	4	2	1		19					265			110		146	411
					109.90	12	6	12-14	9.59		8		22	154	9			4	4			10					263			116		126	389
					110.50	12	6	69-71	9.71		162		3	95	2		2	1				8					363			49		50	413
		C5			111.10	12	6	130-132	9.84	19.81	171		14	92	1			5		1	1	11					355			27		32	387
					111.50	12	7	16.5-18.5	9.92		98		30	120	2			*		1		14					327			40		49	376
			C5n.2n		113.10	13	1	130-132	10.06	20.10	50		9	100	2		1	29				8					372			3		136	508
					114.70	13	2	142-144	10.16	18.93	8		10	142	1		*	2		25		47	3				391			1		76	467
					116.40	13	4	8-10	10.26		47	1	30	47	4		7	3	2	22		11	10				301	1		5		557	858
					117.90	13	5	12-14	10.35	23.66	34		18	76			4	24		8		99		4	8	*	369					88	457
				IV	119.50	13	6	20-22	10.44		25			104			1	7		1		5	3	2			374	6				52	426
					121.10	13	7	31.5-33.5	10.53	20.83	34		19	22	*		8	7		1		25	16	10	3		339			8		71	410
					122.70	14	1	141.5-143.5	10.63	19.69	70		31	17	1		2	12		2		19	24	12	*		352					223	575
					124.30	14	3	4-6	10.72	21.37	20		22	123			4	3		1	3	17	4	3	1		369					42	411
					125.90	14	4	10-12	10.82	22.24	33		12	130	2		1	8		9	6	25	9	6	2		355	3				761	1116
					127.50	14	5	20-22	10.91	20.06	42		6	209	2		2	5			1	12	4	1	4		359	12				757	1116
					129.10	14	6	30-32	11.00	21.46	90		9	155	1			11		*		4	6	3	4		354	9				237	591
			C5r		130.30	14	7	1-3	11.09	19.48	20		34	90	5			22				2	10	11		*	372	7				76	448
					131.50	15	1	74-76	11.19	19.77	75		41	124	2			3				2	10	*		*	368	*				181	549
					132.70	15	2	38-40	11.28	16.57	64		53	62	8		4	7		1	2	4	8	20		18	366	2				26	392
					133.80	15	3	4-6	11.37	22.69	17		17	214	6		2	11		2		6	6	8	1	3	362	2				12	374
					135.00	15	3	123-125	11.47		15		18	221	*		*	*	8		*	1	*	5			375	1				60	435
					136.30	15	4	100-102	11.57	26.02	74		34	96	3		1		3		6	2	4	5		38	383	10				117	500
Middle Miocene	Serravallian				137.50	15	5	74-76	11.67	19.09	16		75	91	4		3	1	2	8	*	2		3		6	352					37	389
					138.70	15	6	37-39	11.76	20.24	36		3	295	*			*					1	*			358					6	364
					139.30	15	6	92-94	11.81	21.22	69		112	30	5		1	3	*		3	1	15	17		1	359				9	24	383
					140.50	16	1	17-19	11.90	24.75	26		232		11		*	1				5	3	3		3	376					156	532
					141.70	16	1	140-142	12.00		19		62	112	17		3	1			*	3		8	6	2	356	1				757	1113
		C5A	C5An		142.70	16	2	91.5-93.5	12.11	24.27	31		162	48	3		1	2		2		*	1				362				3	1033	1395
					143.70	16	3	42.5-44.5	12.21		50		20	73			5	6		1	2	155	2	5		10	363					153	516
					144.70	16	3	141-143	12.32		17		28	188	1		1	7				1	3	*	1	*	361				10	745	1106
			C5Ar		145.70	16	4	92-94	12.42	20.65	29		32	100	15		*	13		1		30	7	*		*	375					104	479
					148.00	16	6	20-22	12.52	21.14	21		32	133	3		4	10		*	13	12	1	21	3	*	368				9	1092	1460
					150.30	17	1	51.5-53.5	12.62		48		59	88	4		3	8		1	8	4	3	*		3	368				1	204	572
					152.60	17	2	130-132	12.71		2		104	205	3			1		*	5	*		*			370					116	486
					154.90	17	4	60-62	12.81	22.08	46		67	137			*	1			11	5		3			367				17	118	485
					157.20	17	5	138-140	12.91		26		128	135	5			4		1	22	6	2	4	1	2	365	2			29	81	446
					159.50	18	1	20-22	13.01		28		182	8	24		*	7		*	2	2	9	34		1	363	1			1	392	755
		C5AA	C5AAn		163.00	18	3	65-67	13.11		20		4	232				2		*	17	8		4		1	362					71	433
			C5AAr		166.50	18	5	121-123	13.26	21.79	9		36	159				11		2	7			3		2	360					161	521
					167.80	18	6	97-99	13.35	20.40			41	192	2			22			6		3	3		*	370	*			18	111	481
		C5AB	C5ABn		169.10	19	1	34-36	13.39		7		8	124				1		*	3	*		2			363	*			3	185	548
					174.70	19	4	138-140	13.49	25.20	9		2	286				1		*	5	*		1			364					6	370
					180.30	20	2	46-48	13.59		3		8	274	*			2			1	1		2		1	355	1				72	427
			C5ABr		185.30	20	5	98-100	13.68				1	333	2									2	2		383					20	403
	Langhian		C5ACn		190.30	21	2	97.5-99.5	13.83		3		12	176						*			*	1	8	*	382	1			11	67	449
					195.30	21	6	2-4	13.94		2		6	308				6		*	8	8	13			*	360				21	68	428
				V	200.30	22	2	147-149	14.03		8		9	33				10			2	212	10			6	360	1				373	733
					205.30	22	6	51-53	14.13		23		11	54				4		1	6	63	8			8	385	1			4	76	461
					210.30	23	3	51.5-53.5	14.23		17		4	162				8		1	25					5	356				39	122	478
					215.30	23	6	97.5-99.5	14.33				10	45				17		5	4	107				2	379				87	300	679
					216.30	23	7	48-50	14.43				10	37				8				104				5	373	4			14	76	449
					216.50	23	CC	10-12	14.53				14	29				10				71				5	347	7			13	122	469

☰	Biosilica	☷	Silty clay

Fig. 2. Raw counts of selected dinocyst and acritarch species (data from Schreck et al., 2013) and their relation to alkenone-based sea surface temperature (data from Schreck et al., 2013; De Schepper et al., 2015; Stein et al., 2016) in ODP Hole 907A. Light shading illustrates the total stratigraphic range and dark shading the first and last occurrence respectively. * = species only encountered outside regular counts, (n) or (*) = suspected reworking. Also shown is the magnetostratigraphy (Channell et al., 1999) and the lithostratigraphic units (Shipboard Scientific Party, 1995) of ODP Hole 907A.

distribution and stratigraphic ranges. Ultimately, our study enhances the application of fossil palynomorph assemblages for paleoenvironmental reconstructions in the Neogene of the Arctic and subarctic seas, and improves our understanding of paleoceanographic implications of assemblages that do not have a modern analogue.

2. Material and methods

2.1. Material

Located on the eastern Iceland Plateau (69°14.989′ N, 12°41.894′ W; 2035.7 m water depth; Fig. 1), ODP Hole 907A was drilled in an undisturbed hemipelagic sequence, terminating at a total depth of 224.1 m below sea floor (Shipboard Scientific Party, 1995). The lithology mainly consists of unlithified silty clay and clayey silt. Five lithostratigraphic units were distinguished based on their siliciclastic, biogenic calcareous, and biogenic siliceous contents (Fig. 2). Unit III is subdivided into Subunit IIIA, which is nannofossil ooze bearing, and Subunit IIIB lacking calcareous nannofossils, but having higher biogenic silica content (Shipboard Scientific Party, 1995).

Previous studies (e.g. Schreck et al., 2012, 2013) used the revised composite magnetostratigraphy of ODP Site 907 (Channell et al., 1999) adjusted to the Astronomically Tuned Neogene Time Scale 2004 (ATNTS 2004, Lourens et al., 2005). Here, we update the paleomagnetic reversals to the Geological Time Scale 2012 (Hilgen et al., 2012), which is identical to the ATNTS 2004 back to 8.3 Ma. The investigated interval spans the entire Pliocene and extends back to the early Middle Miocene. In addition to the 126 samples from Hole 907A, we included five samples from the Pliocene of Hole 907B, resulting in a total of 131 samples analysed for palynology and biomarkers.

2.2. Palynology

Subsamples (~15 cm^3) were processed using standard palynological techniques including acid treatment (cold HCl [10%], cold HF [38–40%]), but without oxidation or alkali treatments (see Schreck et al., 2012 for details). Two *Lycopodium clavatum* tablets were added to each sample during the HCl treatment to calculate palynomorph concentrations (Stockmarr, 1977). The residue was sieved over a 6 μm polyester mesh and mounted with glycerine jelly on microscope slides.

Six samples from Hole 907A (indicated by asterisk on Fig. 2) and the five sample from Hole 907B (not shown on Fig. 2) were processed by Palynological Laboratory Services Ltd. (Holyhead, UK) using a similar processing technique, also without oxidation (details in De Schepper et al., 2017). For those samples, only one *Lycopodium clavatum* tablet was added. The residue was sieved on 10 μm and mounted with glycerine jelly on microscope slides.

Wherever possible, marine palynomorphs have been counted until a minimum of 350 dinocysts had been enumerated. All counts were conducted at 40× and 63× magnification respectively, using a Zeiss Axioplan 2 and Zeiss Axio Imager.A2 microscope. Dinocyst and acritarch nomenclature follows Williams et al. (2017), De Schepper and Head (2008), Schreck et al. (2012), and Schreck and Matthiessen (2013, 2014). However, in contrast to De Schepper and Head (2008), we have not distinguished *Operculodinium*? *eirikianum* on variety level. Percentage calculations for dinocysts (Figs. 3, 5–7) are based on the sum of all cysts counted to ensure comparability with previously published data. The relative abundance of acritarchs (Figs. 3 and 8) is based on the total marine palynomorph assemblage (= dinocysts + acritarchs). To evaluate the reliability of relative abundances as a function of total cyst counts and dissemination of individual species, we have calculated the simultaneous confidence intervals (95%) for each sample following Sison and Glaz (1995; Fig. 4). Except for six samples from Hole 907A (indicated with asterisk on Fig. 2) and five samples from Hole 907B (not shown on Fig. 2), all palynological data have previously been published by Schreck et al. (2012, 2013). These data can be accessed at www.pangaea.de via doi:https://doi.org/10.1594/PANGAEA.805377 and doi:https://doi.org/10.1594/PANGAEA.807134.

2.3. Alkenone paleothermometry

This study uses alkenone SST estimates previously published by Schreck et al. (2013), De Schepper et al. (2015), and Stein et al. (2016), but adds another 11 samples (see above) to the Site 907 SST record (Figs. 2 and 3). All data have been generated in the organic geochemistry laboratory of the Alfred Wegener Institute, Helmholtz Centre for Polar and Marine Research (Bremerhaven, Germany) using the following procedure: bulk sediments (2 to 7 g) from the same samples as used for palynology were extracted using accelerated solvent extraction (DIONEX, ASE 200; 100 °C, 1000 psi, 15 min, solvent dichloromethane). Compounds have been separated by open column chromatography. The composition of alkenones was analysed with a Hewlett Packard HP 6890 gas chromatograph (n = 120 samples) and an Agilent 7890A gas chromatograph (n = 11 samples). Individual alkenone ($C_{37:3}$, $C_{37:2}$) identification is based on retention time and the comparison with an external standard. The instrument stability has been continuously controlled by reruns of the external alkenone standard (extracted from coccolithophore *Emiliana huxleyi* (Lohmann) cultures with known growth temperature) during the analytical sequences. The range of the total analytical error calculated by replicate analyses is < 0.4 °C. The alkenone unsaturation index $U_{37}^{K'}$ and the global core top calibration (Müller et al., 1998) were used to calculate sea surface temperature (SST in °C). We used the Müller et al. (1998) calibration versus summer SSTs. $U_{37}^{K'}$ shows the best statistical relationship to mean annual SST on a global scale (Müller et al., 1998), but coccolithophore production in the modern Nordic Seas is significantly higher (factor of 10) during summer than during autumn to spring due to the availability of light for photosynthesis. This may cause a shift towards a summer bias in temperature (Schröder-Ritzrau et al., 2001; see also discussion below). The summer calibration is similar to the annual mean calibration of Müller et al. (1998) frequently used in the literature, but results in SSTs higher by a constant value of 1.2 °C independent of the $U_{37}^{K'}$ value. The standard error of this calibration is reported as ± 0.055 $U_{37}^{K'}$ units or 1.7 °C. Due to this uncertainty, we only present integral numbers for the alkenone SSTs. Full details of the method and the reliability of the $U_{37}^{K'}$ index in Neogene deposits of the high northern latitudes are discussed in Schreck et al. (2013) and Stein et al. (2016). The alkenone datasets can be accessed at www.pangaea.de via doi:https://doi.org/10.1594/PANGAEA.807107, doi:https://doi.org/10.1594/PANGAEA.848671 and, doi:https://doi.org/10.1594/PANGAEA.855508.

2.4. Comparison database

To test whether extant taxa have a comparable SST distribution in the Neogene as in the modern ocean, we follow the approach of De Schepper et al. (2011) and first compare selected species to the Northern Hemisphere reference database n = 1492 (Fig. 1). In a second step, the n = 1492 database was restricted to 101 samples (n = 101 database) located in the Iceland Sea and adjacent areas (between 67 and 78°N, and between 10°E–20°W) to provide a spatially confined representation of our study site and to exclude sites less suitable for comparison. In both datasets species relative abundance is given as a function of summer and winter SSTs derived from the World Ocean Atlas 2001 (WOA01, Stephens et al., 2002). For the purpose of this study, we use the summer (July–September) SSTs given in the WOA01 for comparison as dinoflagellate and coccolithophore

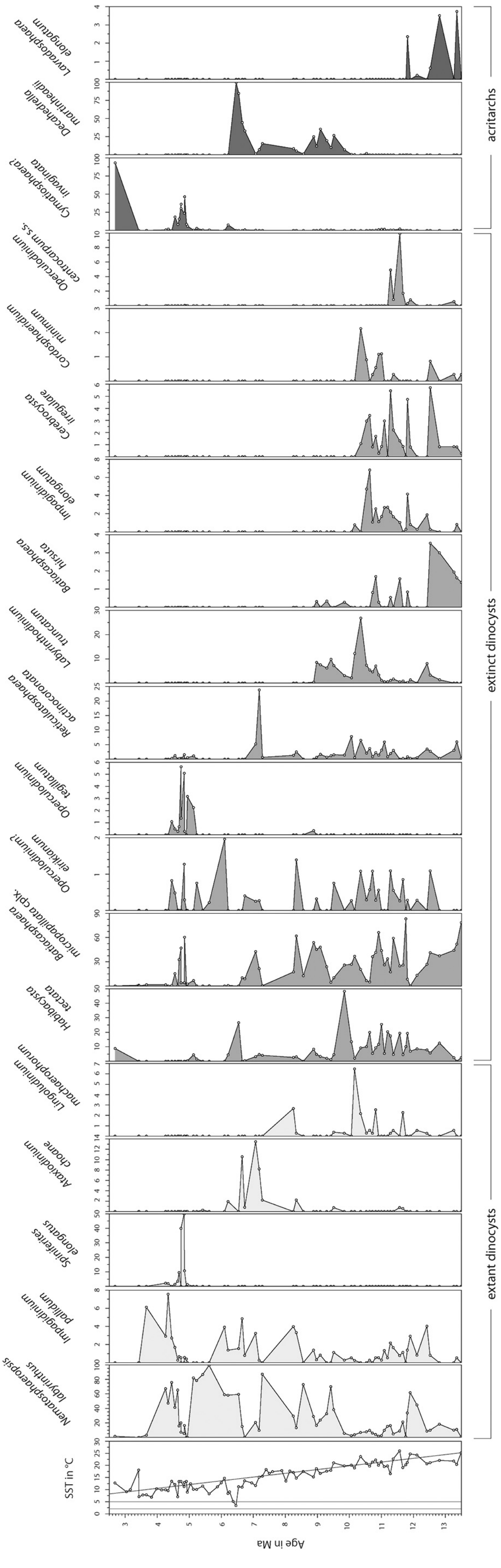

Fig. 3. Relative abundance of extant and extinct dinoflagellate cysts and acritarchs in ODP Site 907. Also shown is the reconstructed alkenone sea surface temperature (SST in °C). Black line depicts the gradual cooling trend observed in ODP Site 907. Red line presents the present-day sea surface temperature in the study area, while the blue line presents the present-day annual mean sea surface temperature. (For interpretation of the references to colour in this figure legend, the reader is referred to the web version of this article.)

production in the Nordic Seas today is mainly restricted to the summer season (e.g. Matthiessen et al., 2005; see discussion below). We refrain from a detailed comparison with the global dataset of modern cyst distribution (Zonneveld et al., 2013), which presently consists of 2405 data points (including the Northern Hemisphere reference database), as it contains sites less suitable for meaningful comparison with our high latitude data.

In addition, the distribution of extant and extinct dinocyst species is compared to the North Atlantic paleo-database of De Schepper et al. (2011) where possible. This dataset compares Plio-Pleistocene dinocyst relative abundances with (spring–summer) SST estimates derived from the same sample by measuring Mg/Ca ratios on the planktonic foraminifera *Globogerina bulloides* (d'Orbigny). It currently comprises 204 samples (n = 204 paleo-database) from four DSDP/ODP/IODP sites in the North Atlantic (Fig. 1) spanning the Late Pliocene through Early Pleistocene, and can be accessed at www.pangaea.de via doi:https://doi.org/10.1594/PANGAEA.758713.

For most dinocyst species discussed here, however, no previous calibration of relative abundance vs. SST is available. This also applies to the acritarch taxa presented.

2.5. Comparability of proxies and general limitations of the approach

The approach used here, i.e. combining marine palynomorph assemblages with geochemical SST reconstructions, has previously been proposed by De Schepper et al. (2011). The authors show that extant species (both dominant and less abundant) occurring in fossil assemblages have a similar temperature distribution compared to today, and that these SST reconstructions can therefore be used to assess temperature ranges of extinct species. In contrast to the study of De Schepper et al. (2011), who used the Mg/Ca ratio of planktonic foraminifera *Globogerina bulloides* as a SST proxy, the virtual absence of planktonic foraminifera in the Miocene-Pliocene section of ODP Site 907 (Shipboard Scientific Party, 1995) prevents the application of the same SST proxy for calibration of species relative abundance. However, previous studies have shown that the alkenone unsaturation index $U_{37}^{K'}$ can be applied to reliably reconstruct SSTs on pre-Quaternary timescales at high northern latitudes (see discussion in Schreck et al., 2013; Stein et al., 2016; Herbert et al., 2016).

While sea surface temperature is the primary ecological factor determining the distribution of dinoflagellates (e.g. Taylor, 1987), we note that the relationship between temperature and phytoplankton species abundance might be more complex. In order to compare dinoflagellate cyst abundance, alkenone-based SSTs (this study) and Mg/Ca SSTs (De Schepper et al., 2011), the producing organisms (dinoflagellates, coccolithophores, foraminifera) should have comparable habitat depth and seasonality, as these parameters determine the recorded signal.

2.5.1. Habitat depth

All dinocysts discussed here are cysts of phototrophic dinoflagellate species because of fluorescent properties of the cyst wall (cf. Brenner and Biebow, 2001). Apart from temperature, phototrophic dinoflagellates respond to light availability, and consequently they are restricted to the photic zone of the surface waters. Although capable of vertically adjusting their position in the water column, they generally inhabit a shallow and thin surface layer (e.g. Dale, 1996).

Alkenones are biosynthesized by haptophytes (e.g. coccolithophores, Herbert, 2003) and, given their phytoplanktonic source, the alkenone production must originate from the photic zone. Direct measurements of alkenones in the upper water column indicate that the zone of maximum alkenone production is in the isothermal surface mixed layer (0–20 m) rather than within the deeper chlorophyll maximum layer (e.g. Rosell-Melè and McClymont, 2007, and references therein). Indeed, calibration of the $U_{37}^{K'}$ is best when using temperatures from 0 to 10 m water depth (Müller et al., 1998), suggesting that temperatures derived from alkenone producing coccolithophores reflect surface conditions.

The planktonic foraminifer *Globogerina bulloides* generally occupies a habitat restricted to the upper 60 m in the North Atlantic (Ganssen and Kroon, 2000; Chapman, 2010) and the average calcification depth lies around ± 50 m (Vázquez-Riveiros et al., 2016). Therefore, this species records slightly deeper surface water conditions compared to alkenones.

2.5.2. Seasonality of production

In the Nordic Seas, a generally restricted production period has been observed and the export of fossilizable plankton groups (including dinoflagellates, coccolithophores, foraminifera) occurs during 4–6 months of the year. Hence, the signal recorded in the sediments mainly represents the summer to autumn seasons (Schröder-Ritzrau et al., 2001, and references therein).

While studies of dinocysts in surface sediments are numerous, sediment trap studies focussing on the seasonal production of dinoflagellates and their cysts are rare. Most studies are limited to coastal marine environments, upwelling regions and very restricted marine settings such as fjords and inlets. While on global scale dinoflagellate cyst relative abundance in surface sediments shows a good correlation to summer, autumn and annual mean SSTs (Zonneveld et al., 2013), in the Arctic and Subarctic realm dinoflagellates undergo a pronounced seasonal cycle in production. They are most abundant during summer due to the prevailing light regime and nutrient availability, but never during the spring bloom (see Matthiessen et al., 2005, and references therein). Indeed, the few sediment trap studies from the high latitudes revealed a trend towards summer production of dinoflagellate cysts (e.g. Dale and Dale, 1992; Howe et al., 2010; Heikkilä et al., 2016). Therefore, we consider dinoflagellate cysts as recorders of summer surface conditions in the study area.

The same limitations as discussed for dinocysts also apply to production of coccolithophores in high latitude settings. In the modern Nordic Seas, the production of coccolithophores is significantly higher (factor of 10) during summer than in the non-production period from late autumn to early summer due to the availability of light for photosynthesis (Andruleit, 1997; Schröder-Ritzrau et al., 2001). High cell densities are usually not observed before August (Samtleben et al., 1995). This is also documented by the vertical flux of coccolithophores recorded in sediment traps (Samtleben and Bickert, 1990). Therefore, we interpret the alkenone-derived SSTs to reflect summer SSTs in the study area.

The foraminifer *Globogerina bulloides* reflects the northward migrating North Atlantic spring bloom, February–March between 30° and 40°N, and May–June at higher latitudes (Ganssen and Kroon, 2000). In fact, recently published isotopic temperatures suggest *G. bulloides* to calcify their tests during the summer season between 40 and 60°N (Vázquez-Riveiros et al., 2016). In the eastern North Atlantic it reaches highest abundances in late spring and summer (Chapman, 2010). Therefore, De Schepper et al. (2011) discussed this species as a recorder of spring to summer SSTs in the North Atlantic n = 204 paleo-database. The SST estimates presented by De Schepper et al. (2011) are derived using the North Atlantic calibration of Elderfield and Ganssen (2000).

2.5.3. Limitations of the approach

Despite the fact that dinoflagellate cysts and alkenone producing coccolithophores have a comparable habitat and seasonality in the study area, certain limitations apply to this approach. In particular, dispersal with ocean currents has to be considered when comparing fossil and modern species distribution (Dale and Dale, 1992), but also alkenone distribution (e.g. Mollenhauer et al., 2005). The East Greenland current flowing along the Greenland continental shelf and slope is the main oceanographic feature influencing the Iceland Sea (e.g. Blindheim and Østerhus, 2005). Its north to south configuration limits lateral transport from the Greenland fjords and shelf into the open waters of the study site. Indeed, palynological assemblages of ODP Site 907 indicate an open ocean environment throughout most of the analysed interval with only occasional input from the outer shelf (Schreck et al., 2013; De Schepper et al., 2015). Thus, ODP Site 907 reflects local conditions with only minimal influence by oceanic transport. Another bias to the fossil assemblage may be introduced by species-selective degradation (e.g. Zonneveld et al., 2008). However, this factor does not exert a major influence on the ODP Site 907 palynomorph assemblages in the productive intervals of both the Miocene and the Pliocene (see Schreck et al., 2013 for discussion). Finally, the overall SST range reconstructed for ODP Site 907 (3–26 °C) is largely comparable to that in the present-day n = 1492 database (-1.8–30.5 °C, de Vernal et al., 2013) and the Plio-Pleistocene North Atlantic paleo-dataset (7.7–25.2 °C, De Schepper et al., 2011). However, our dataset contains more samples from the presumably warmer Middle to Late Miocene than from the cooler Pliocene, thus partially introducing an offset towards higher SSTs when compared to the modern n = 1492 and n = 101 reference datasets (de Vernal et al., 2013). Therefore, we may record the warm end of species distribution rather than its minimum SST requirements. Due to these limitations, we refrain from defining exact upper and lower temperature limits for the occurrence of extinct species, but rather provide temperature ranges in which extinct species occurred based on independently derived SST estimates. We note that additional data from different sites needs to be incorporated into the developing paleo-database to allow for more precise assessment of species temperature affinities.

3. Results and discussion

3.1. Alkenone sea surface temperatures

The alkenone SST data used here represent a stack record of data previously published by Schreck et al. (2013), De Schepper et al. (2015) and Stein et al. (2016). They are discussed in detail in the respective publications. In addition, this study adds 11 samples with alkenone-based SST estimates to the ODP Site 907 record. In summary, 86 of the 131 analysed samples yielded sufficient alkenones to allow the application of the $U_{37}^{K'}$ index to calculate summer SST. The $U_{37}^{K'}$ index varies from 0.116 to 0.863, which translates into SSTs ranging from 3 to 26 °C (Figs. 2–3). Modern mean annual SSTs are 2 °C at the study site while summer SSTs are 5 °C (Fig. 3). Thus, the ODP Site 907 record suggests warmer than present-day conditions throughout most of the analysed interval. Highest temperatures are observed in the Middle Miocene. SSTs subsequently decrease towards the end of the latest Pliocene (Figs. 2–3), where SSTs close to modern values have been recorded. The long-term temperature evolution in the Iceland Sea therefore follows the general global Neogene cooling trend (Zachos et al., 2008). However, samples with low amounts of alkenones preventing a reliable calculation of the $U_{37}^{K'}$ index cluster in the early Middle Miocene (Langhian stage) and latest Pliocene. The Late Pliocene interval coincides with samples almost barren of palynomorphs (Figs. 2–3; Schreck et al., 2013) and diatoms (Stabell and Koç, 1996), which has been assigned to a combination of factors such as sea ice cover, nutrient availability, bottom water ventilation and selective degradation in relation to waxing and waning of the Greenland Ice Sheet. That may also account for the low amounts of alkenones. In contrast, the Langhian (Middle Miocene) samples are characterized by high palynomorph and diatom abundance and diversity, so that the controlling factors for the low alkenone abundance remains speculative.

3.2. Dinoflagellate cysts and acritarchs

The details and raw data of the palynological investigation are presented in Schreck et al. (2013) and summarized together with our new data in Figs. 2–3. Several species exhibit restricted stratigraphic ranges with well-defined range tops. This is exemplified in clusters of highest occurrences (HO) in the early Late Miocene and Early Pliocene (Figs. 2–3). From the 86 samples with SST estimates (see above) 18 were virtually barren (< 50 palynomorphs counted, Fig. 2). These 18 samples have been removed from the dataset due to the large statistical uncertainty introduced by the low number of counts. Of the remaining 68 samples, 48 samples yielded > 350 cysts while 7 samples contained < 150 cysts (Figs. 2 and 4). In order to account for the variability in the number of counts per sample and to evaluate the statistical error it introduces, we have calculated the simultaneous confidence interval (95%) for each sample using the method of Sison and Glaz (1995), which takes the total number of counts per sample into account, but also the distribution of counts for each individual species. This corresponds to confidence intervals on the relative abundance of ± 0.6 to ± 12.9% in any given sample, and an average of 5.3% on the entire dataset (Fig. 4). In general, higher count numbers result in smaller confidence intervals (represented by larger dots in Figs. 5–8) and are thus more reliable. This allows to objectively assess the reliability of the relative abundance and avoid overinterpretation.

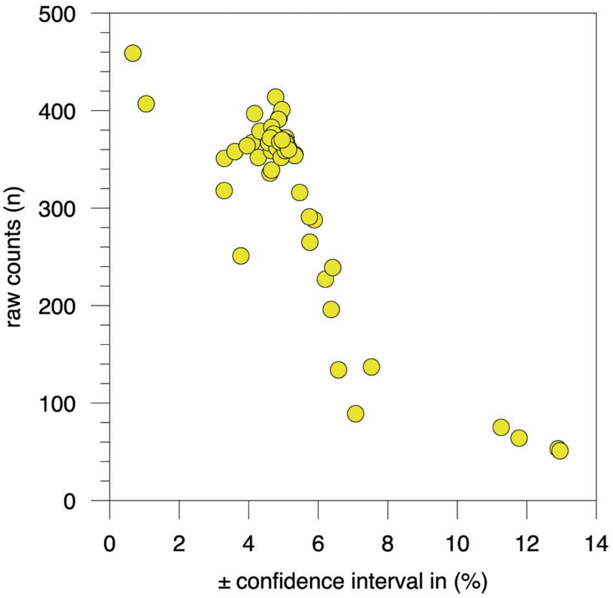

Fig. 4. The calculated simultaneous confidence interval (95%) using the method of Sison and Glaz (1995) for all samples in our Miocene-Pliocene database (n = 68). Samples with < 50 palynomorph counts have been omitted from that figure.

In summary, this study provides 68 samples with marine palynomorph relative abundance calibrated to SST estimates from the Miocene through Pliocene. The temperature affinities of extinct species discussed in the text are summarized in Fig. 9.

3.3. Extant dinoflagellate cysts

Even though extant species are recorded almost continuously in the Middle Miocene to Late Pliocene of ODP Site 907, their relative abundances are usually low (< 1%) thus rendering conclusions on their paleoecology difficult. Extant species recorded include *Bitectatodinium tepikiense*, *Impagidinium aculeatum*, *Impagidinium patulum*, *Impagidinium strialatum*, *Operculodinium israelianum*, *Selenopemphix nephroides*, *Tectatodinium pellitum* and several *Brigantedinium* species. Only *Nematosphaeropsis labyrinthus*, *Impagidinium pallidum*, *Ataxiodinium choane*, *Spiniferites elongatus* s.l. and *Lingulodinium machaerophorum* occur continuously and in higher relative abundances (up to ~80%) in parts of the analysed interval, and are hence discussed here (Fig. 5). Species abundance is plotted against alkenone-based SSTs (yellow dots) and compared with their modern distribution in the Northern Hemisphere reference dataset (black and grey dots) and the n = 101 subset (grey dots only). The present-day data are plotted as a function of summer SST derived from the WOA01 (Stephens et al., 2002) because they provide the best comparison with our alkenone-based SSTs, which reflect summer temperatures at the study site (see discussion above). In addition, we compare the Miocene-Pliocene species distribution with that observed in the n = 204 paleo-dataset from the Plio-Pleistocene North Atlantic (blue dots), where species relative abundance is plotted against Mg/Ca spring-summer SST (De Schepper et al., 2011).

At ODP Site 907, *Lingulodinium machaerophorum* is restricted to the comparatively warm Miocene, where it occurs at SSTs ranging from 15 to 24 °C (Fig. 5). This compares favourably with its distribution in the present-day n = 1492 database, where it is restricted to SSTs between 14 and 30 °C (de Vernal et al., 2013), and also with its distribution in the Plio-Pleistocene North Atlantic, where it mainly occurs between 16 and 24 °C (De Schepper et al., 2011). *Lingulodinium machaerophorum* is a temperate to tropical species

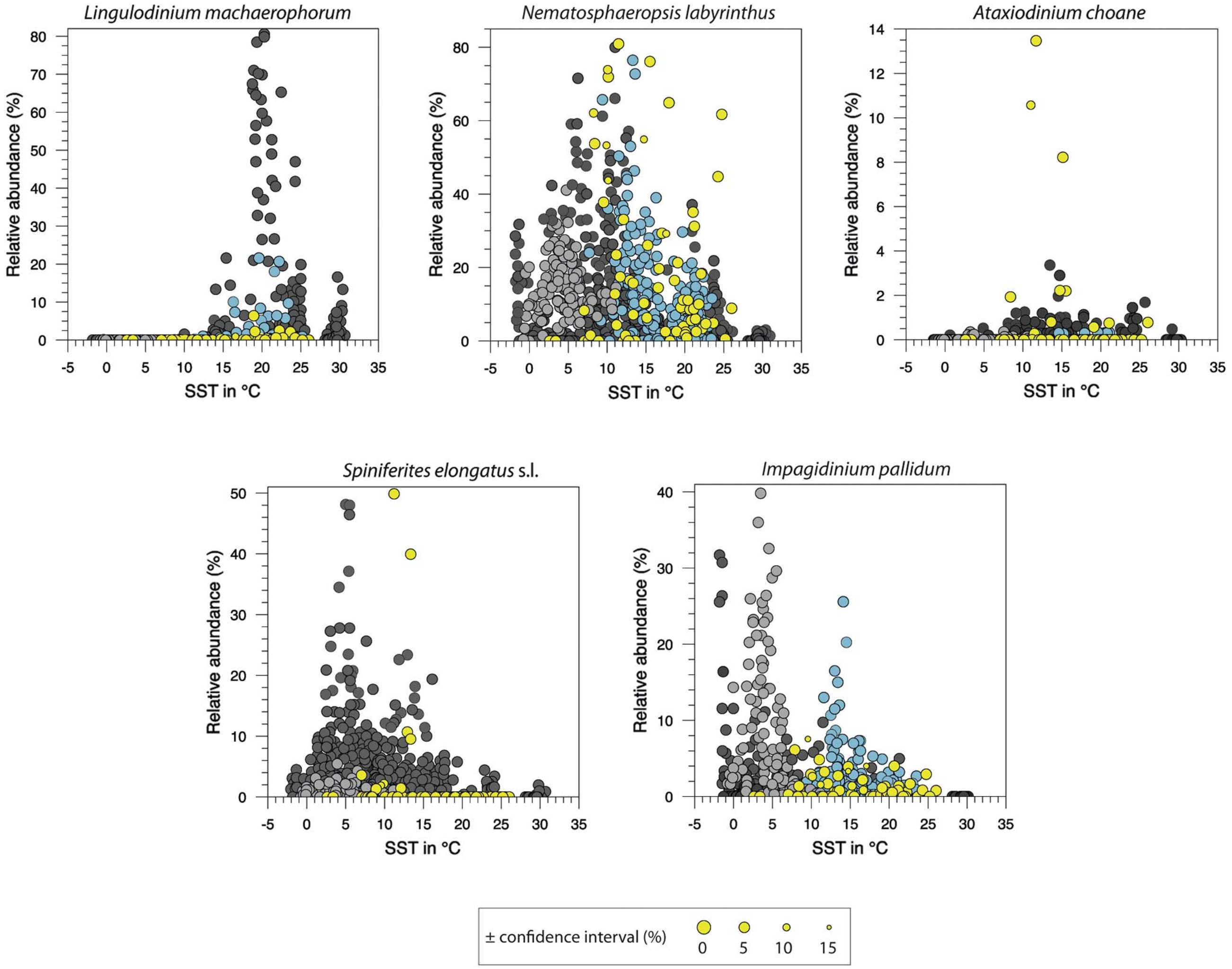

Fig. 5. Relative abundance (in %) of extant dinoflagellate cysts in relation to sea surface temperatures (SST in °C). Species relative abundance (yellow dots) is plotted against alkenone-based SST. Species relative abundance in the modern ocean (n = 1492 = black and grey dots, n = 101 = grey dots only) is plotted against present-day summer SST derived from the World Ocean Atlas 2001 (Stephens et al., 2002). For the Pliocene-Pleistocene n = 204 paleo-database (blue dots) species relative abundances are plotted vs. foraminiferal Mg/Ca-derived (spring-summer) SST (De Schepper et al., 2011). (For interpretation of the references to colour in this figure legend, the reader is referred to the web version of this article.)

today (Zonneveld et al., 2013) and accordingly has not been observed in the n = 101 subset from the Nordic Seas, where present-day summer SSTs are around 5 °C. It is only a minor component of the ODP Site 907 dinocyst record and thus the data has to be treated with caution due to the uncertainties related to the low numbers of counts. However, our paleo-dataset suggests a preference for warm waters during the Neogene in accordance with its present-day and its Plio-Pleistocene distribution, indicating a similar lower limit on its occurrence as observed today (> 15 °C).

Nematosphaeropsis labyrinthus exhibits a broad temperature range in both the Mio-Pliocene Iceland Sea (7–26 °C, Fig. 5) and the modern ocean (-1.8–30 °C). Its Neogene distribution compares particularly well at the warm end of its temperature distribution with both present-day datasets (n = 1492 and n = 101), but clearly misses elevated relative abundances below 5 °C. A similar distribution is observed in the n = 204 paleo-database (De Schepper et al., 2011), which compares favourably with our data. However, both paleo-datasets (n = 204 and this study) do not facilitate comparison at the lowermost end of this species present day SST range as they only contain two samples with temperatures < 5 °C compared to the strong representation of this temperature interval in the modern dataset. Nonetheless, it is interesting to note that *N. labyrinthus* becomes successively more abundant over the course of the gradual Neogene cooling observed in ODP Hole 907A (Fig. 3). Besides few exceptions, however, relative abundances > 40% are confined to the interval from 8 to 15 °C in both paleo-datasets, while such relative abundances are observed between 7 and 12 °C in the present-day distribution of this cosmopolitan species.

Ataxiodinium choane occurs in subpolar to temperate regions of the Northern Hemisphere today and has been rarely observed in the Southern Hemisphere (Zonneveld et al., 2013). In the Mio-Pliocene of the Iceland Sea, it occurs at temperatures ranging from 8 to 21 °C, exceptionally as high as 26 °C, which is similar to its present-day distribution in the n = 1492 database (0–25 °C, Fig. 5, de Vernal et al., 2013), in particular at the warm end of its temperature distribution. It can apparently occur at lower temperatures today (< 5 °C) but then it is only rare (< 1%). *Ataxiodinium choane* accounts for up to 3% of the modern dinocyst assemblage, but constitutes as much as 8–14% of the dinocyst assemblage in the Neogene of the Iceland Sea. It is important to note that its maximum relative abundance at the study site is related to similar SSTs (10–15 °C) as its maximum abundance in the modern ocean, thus lending confidence to our reconstruction. In the Plio-Pleistocene North Atlantic, this species is only a rare component of the dinocyst assemblage (< 0.5%, data supplement in De Schepper et al., 2011), but it occurs at temperatures ranging from 11 to 21 °C in the n = 204 paleo-database, thereby more or less supporting our Mio-Pliocene temperature assessment.

In the modern ocean, *Spiniferites elongatus* s.l. is a polar to subtropical species restricted to the Northern Hemisphere (Zonneveld et al., 2013). It occurs at SSTs ranging from -1.8 to 25 °C (Fig. 5), occasionally as high as 30 °C, but has highest relative abundances (> 10%) between 2 and 15 °C (de Vernal et al., 2013). At ODP Site 907, *S. elongatus* s.l. is mainly confined to the cooler Pliocene interval and is present in only two samples from the Miocene. It occurs at restricted SSTs between 7 and 13 °C, and is particularly abundant between 5 and 4 Ma when ODP Site 907 received increased IRD input (Fronval and Jansen, 1996), which may suggest a tolerance for colder surface waters similar to its present-day distribution.

In contrast, the Middle Miocene to Pliocene record of *Impagidinium pallidum* suggests a preference for warmer conditions than its distribution in the modern ocean. Today this species occurs at SSTs ranging from − 2.1 to 25.7 °C (Zonneveld et al., 2013), but is most abundant (> 10% of the assemblage) in the Northern Hemisphere at SSTs ranging between − 1.8 and 6.5 °C, clearly suggesting a cold-water affinity (Fig. 5, de Vernal et al., 2013). This species apparently has a similar overall SST range (7–26 °C) and reaches highest relative abundance (6–8% of the assemblage) at the colder end of its temperature spectrum (7–10 °C) in the Mio-Pliocene Iceland Sea, but does not exhibit increased abundances at similarly lower temperatures as observed in the present-day database. In fact, *I. pallidum* never constitutes more than 10% of the dinocyst assemblage at ODP Site 907, which is in contrast to its high relative abundance in the present-day Iceland Sea (Matthiessen, 1995; Marret et al., 2004). The overall temperature range in the Iceland Sea agrees well with the distribution observed in the Plio-Pleistocene North Atlantic and, in particular, its occurrence at temperatures exceeding 15 °C supports the tolerance of *I. pallidum* for higher SSTs in the past as suggested by De Schepper et al. (2011). However, De Schepper et al. (2011) reported highest relative abundances (> 10%) of *I. pallidum* at SST values between 10 and 15 °C only at DSDP Site 610 from the eastern North Atlantic, while in the Iceland Sea it reaches maximum relative abundance at SSTs between 7 and 10 °C, thus being closer to present-day values. Nonetheless, the occurrence of *I. pallidum* at warmer conditions in the geological past, in particular in the eastern North Atlantic, is in clear contrast with its present-day distribution (Fig. 5), which suggests other factors, such as nutrient availability, may play a decisive role in controlling its abundance. While its present-day distribution reflects affinities with cold and rather oligotrophic environments this might have been different in the past. However, we note that the modern database does not include warm oligotrophic sites. It is worth mentioning, that *I. pallidum* is stratigraphically long-ranging and extends back into at least the Middle Eocene (Bujak, 1984; Head and Norris, 1989). Its existence during those periods, which were much warmer than today, already suggests some tolerance for warmer conditions. Moreover, its longevity also suggests a potential for adaption to changing environments. However, given the fact that *I. pallidum* reaches highest relative abundances in the present-day Nordic Seas and the eastern Arctic Ocean (Matthiessen, 1995), reduced habitat competition in these hostile environments may also explain the observed differences. On the other hand, it may also reflect the existence of two cryptic species and therefore explain the observed differences in distribution. We therefore corroborate the questionable value of *I. pallidum* as a reliable cold-water indicator in older (pre-Quaternary) deposits (this study, De Schepper et al., 2011).

3.4. *Extinct dinoflagellate cysts*

The majority of the Miocene to Pliocene samples of ODP Site 907 is dominated by extinct species. Despite the high diversity of the palynomorph record, however, only 10 dinocyst species continuously occur in significant numbers to reliably perform a correlation exercise. Most species are rare (< 2% of the assemblage) or occur in a few samples only (see Schreck et al., 2013 for details), thus conclusions on their ecological affinities. Therefore, only the most relevant species are shown in Figs. 6–7 and 9, and discussed here. All Miocene to Pliocene data (yellow dots) are plotted versus alkenone-derived summer SSTs. *Habibacysta tectata* and *Operculodinium*? *eirikianum* have also been recorded by De Schepper et al. (2011) from the Plio-Pleistocene North Atlantic, hence allow to compare their distribution with the n = 204 paleo-database (Fig. 6).

Based on its geographical distribution in the Pliocene of the Labrador Sea, North Atlantic and North Sea basin, *Habibacysta tectata* has been considered a cool-water tolerant (Head, 1994) to cold-water species (Versteegh, 1994), while recent quantitative data indicate a broader temperature tolerance with a cool-water affinity (De Schepper et al., 2011; Hennissen et al., 2017). This species has also been recorded from the Middle Miocene of the Mediterranean (Jiménez-Moreno et al., 2006), and the upper Miocene of the Gulf of Mexico (as *Tectatodinium* sp. B in Wrenn and Kokinos, 1986) and the Caribbean Sea (Wrenn pers. com. in Head, 1994) respectively, suggesting a much wider thermal preference. In Iceland Sea ODP Hole 907A, which covers both the Miocene and the Pliocene, *H. tectata* indeed exhibits a much broader temperature range (8–26 °C, Figs. 6 and 9) than in the study of De Schepper et al. (2011, 11–17 °C), suggesting that temperature may not be the only factor controlling this species distribution. Even though it can occur at temperatures below 10 °C, it clearly shows a centre of distribution at temperatures > 15 °C. Given its wide temperature distribution across the Middle Miocene to Pliocene in the Iceland Sea (this study), its more restricted range in the Plio-Pleistocene North Atlantic and its overall biogeographic distribution ranging from subtropical/tropical (in the Miocene) to subpolar (in the Plio-Pleistocene), this may suggest an adaptation of this species towards cooler conditions occurring in concert with the general global cooling observed during the Neogene, with optimum temperatures > 15 °C. Based on the clear decrease in relative abundance around 10 °C, and comparable to the conclusion of Hennissen et al. (2017) we consider *H. tectata* as a cold-

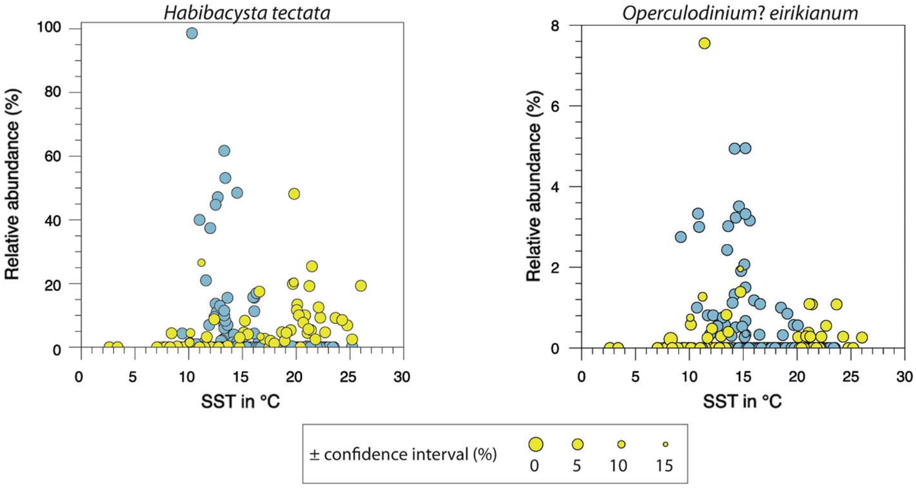

Fig. 6. Relative abundance (in %) of extinct dinoflagellate cysts in relation to sea surface temperatures (SST in °C). Species relative abundance (yellow dots) is plotted against alkenone-based SST, and for the Pliocene-Pleistocene n = 204 paleo-database (light blue dots) species relative abundance is plotted vs. foraminiferal Mg/Ca-derived (spring-summer) SST (De Schepper et al., 2011). (For interpretation of the references to colour in this figure legend, the reader is referred to the web version of this article.)

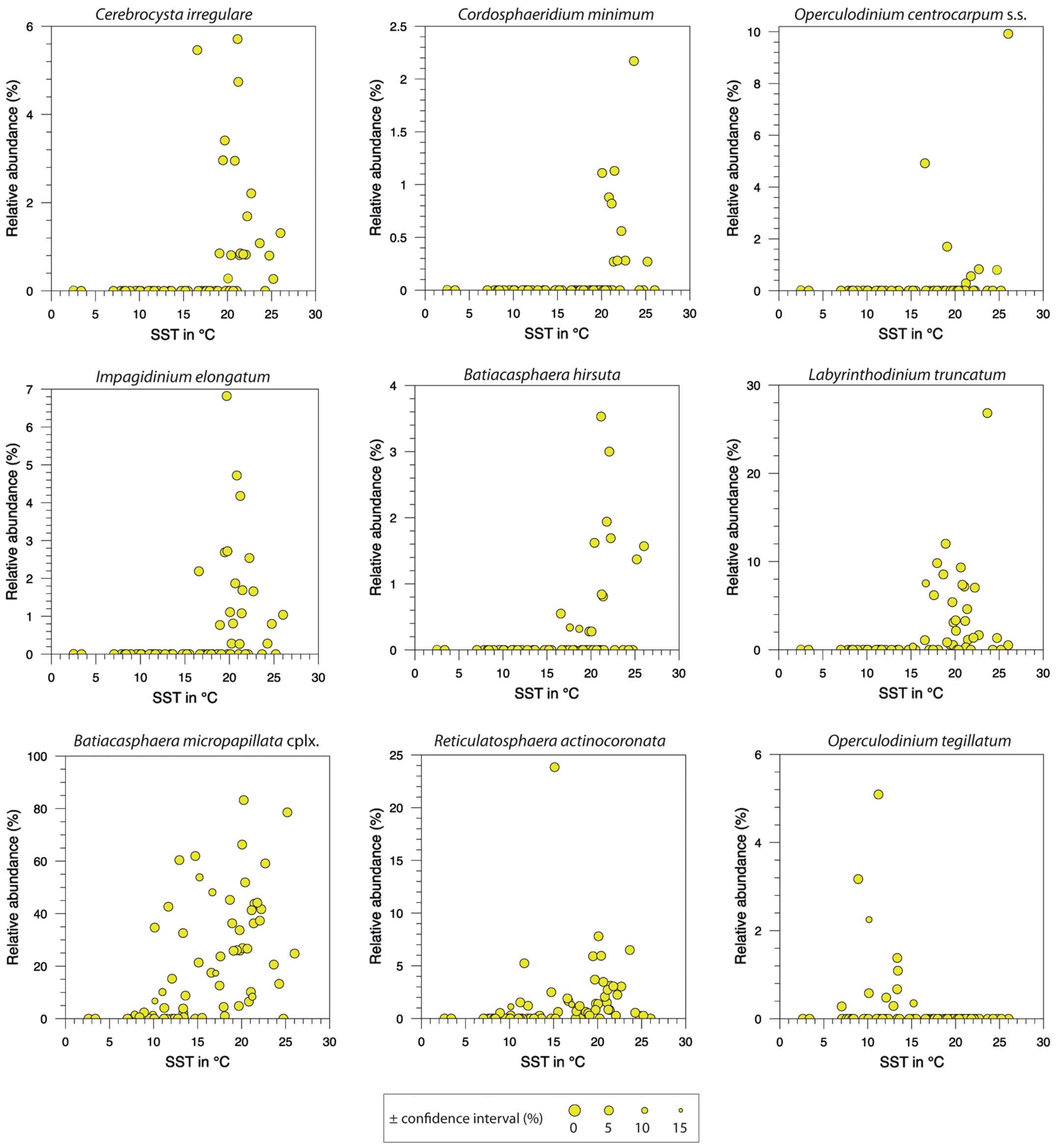

Fig. 7. Relative abundance (in %) of extinct dinoflagellate cysts in relation to sea surface temperatures (SST in °C). Species relative abundance (yellow dots) is plotted against alkenone-based SST. (For interpretation of the references to colour in this figure legend, the reader is referred to the web version of this article.)

tolerant species rather than a strictly cold-water indicator.

Operculodinium? *eirikianum* is only a minor component of the Mio-Pliocene palynomorph assemblage in the Iceland Sea, and thus conclusions should be treated with caution. However, similarly low counts of *O.*? *eirikianum* have been reported from the Miocene and Pliocene of the North Atlantic and North Sea basin suggesting this species is typically a minor but consistent component of Neogene assemblages (e.g. Louwye, 2002; Louwye et al., 2007; Louwye and De Schepper, 2010; De Schepper et al., 2011; Quaijtaal et al., 2014). It is present from 8 to 26 °C in the Mio-Pliocene of the Iceland Sea (Figs. 6 and 9), but in significant numbers (> 5%) only in one sample at 12 °C, thus clearly restricting interpretations of its paleoecological preferences. Nonetheless, the lower limit of distribution compares well with the n = 204 North Atlantic paleo-database where both subspecies (*O.*? *eirikianum* var. *eirikianum* and *O.*? *eirikianum* var. *crebrum*) have not been recorded at SSTs below 9 °C (De Schepper et al., 2011). This may suggest a certain temperature threshold on its occurrence and supports the interpretation of this species being cold-intolerant (Head, 1997).

The species stratigraphically restricted to the Miocene (*Cerebrocysta irregulare*, *Cordosphaeridium minimum*, *Operculodinium centrocarpum* s.s., *Impagidinium elongatum*, *Batiacasphaera hirsuta*, and *Labyrinthodinium truncatum*) all show a preference towards higher temperatures (Figs. 7 and 9). *Cerebrocysta irregulare*, *Cordosphaeridium minimum*, *Operculodinium centrocarpum* s.s. and *Impagidinium elongatum* are all confined to the early Late Miocene and occur at SSTs between 19 and 26 °C, with only one sample recorded at a lower temperature (16 °C) outside this restricted SST range. All four species disappear around 10.5 Ma when temperatures permanently drop below 20 °C (Figs. 2–3). In addition, siliciclastic sedimentation becomes predominant and the first drop stone is recorded at the study site (Shipboard Scientific Party, 1995). This suggests incisive environmental changes in the study area causing these species to disappear. It seems likely that a critical temperature threshold on the occurrence of these species might have been crossed, but a lower temperature limit cannot be assessed with certainty based on the limited data available. Similarly, *Batiacasphaera hirsuta* persistently occurs with relative abundances > 1% of the dinocyst assemblage at SSTs in excess of 20 °C (Fig. 7). In contrast to *C. irregulare*, *C. minimum*, *O. centrocarpum* s.s., and *I. elongatum*, which all disappear around 10.5 Ma, *B. hirsuta* still occurs, although sporadically and in very low numbers only, at temperatures as low as 16 °C until its HO in ODP Hole 907A at around 8.5 Ma (Figs. 2–3). *Labyrinthodinium truncatum* clearly shows a centre of distribution at SSTs between 16 and 22 °C, occasionally occurring at even higher temperatures (Figs. 7 and 9). It has a similar stratigraphic range as *B. hirsuta*, but in contrast to the latter it occurs continuously and in greater numbers until its HO around 8.5 Ma (Fig. 3). While the contemporaneous disappearance suggests a similar temperature threshold for the occurrence of both species, *L. truncatum* appears to be more tolerant towards cooler conditions than *B. hirsuta* judged by its higher relative abundances.

All six Miocene species exhibit very restricted temperature ranges in ODP Hole 907A, but with distinctively varying thermal affinities indicating a strong individual adaptation to the warm conditions prevailing during most of the Miocene. *Cerebrocysta irregulare*, *C. minimum*, *O. centrocarpum* s.s. and *I. elongatum* disappear in an interval when the first drop stone is observed and temperatures constantly drop below 20 °C, suggesting an intolerance towards cooler conditions. *Batiacasphaera hirsuta* and *L. truncatum* occur at SSTs as low as 16 °C, the latter probably being more tolerant to these temperatures judged by its higher relative abundances. However, none of the six taxa have been recorded at temperatures lower than 15 °C clearly suggesting them all to be warm-water species. They all disappear from the Nordic Seas and the North Atlantic in the early Late Miocene in concert with general Neogene climate deterioration (Figs. 2–3).

In contrast, the *Batiacasphaera micropapillata* complex and *Reticulatosphaera actinocoronata*, which both range up into the Early Pliocene across the North Atlantic, occur at a much broader temperature range (Figs. 7 and 9). The *B. micropapillata* complex ranges from 8 to 26 °C, but highest relative abundances are recorded at the warm end of the SST spectrum reconstructed for Iceland Sea ODP Site 907. It contributes to the dinocyst assemblage at temperatures below 10 °C, but relative abundance only starts to increase at SSTs > 10 °C. Previous interpretations of this species complex as being warm- to cool-temperate based on its (paleo) biogeographic distribution (Schreck and Matthiessen, 2013) may have to be reconsidered since high relative abundances at SSTs in excess of 15 °C clearly suggests a warm water affinity. *Reticulatosphaera actinocoronata* has a similar temperature range and occurs at SSTs between 9 and 25 °C. Relative abundances of 2.5% and above are usually associated with SST values > 18 °C and it only occurs sporadically at temperatures lower than 15 °C. This indicates a lesser tolerance of this species versus colder waters compared to the *B. micropapillata* complex, which is still common (e.g. > 10%) at SSTs between 10 and 15 °C (Fig. 3). In addition, *R. actinocoronata* disappears earlier than the *B. micropapillata* complex across the North Atlantic during Pliocene cooling supporting the interpretation of *R. actinocoronata* being less tolerant towards colder conditions. However, both taxa tolerate a wide range of temperatures, thus favouring their cosmopolitan distribution in the Neogene (see Schreck et al., 2012, and references therein). They disappear in the Iceland Sea during the Early Pliocene in concert with a fundamental reorganisation of the Nordic Seas surface circulation (Schreck et al., 2013; De Schepper et al., 2015).

Operculodinium tegillatum is only a minor constituent of the dinocyst assemblage at ODP Site 907, and interpretations should thus be considered tentative. It is largely confined to the Early Pliocene interval and only occurs sporadically in the warmer Miocene (Figs. 2–3). It exhibits a restricted temperature range and its occurrence is related to SSTs between 7 and 15 °C (Figs. 7 and 9), indicating a tolerance versus cool-temperate conditions. We note, however, that occurrences at both ends of the temperature spectrum are confined to very low relative abundances. Contemporaneously with *B. micropapillata* and *R. actinocoronata*, this species disappears at 4.5 Ma from the record of ODP Hole 907A (Fig. 3). This disappearance event has been related to a general reorganisation of surface water circulation in the entire Nordic Seas (De Schepper et al., 2015). As these changes in oceanographic conditions certainly affected different surface water mass properties, it leaves the question whether species disappearance is exclusively a function of temperature (e.g. cooling). As all three species have slightly different thermal preferences it seems likely that other factors such as salinity and nutrient availability also played a crucial role in their coeval disappearance.

3.5. Acritarchs

Due to their small size, unknown biological affinity and challenging taxonomy, acritarchs have often received considerably less attention than dinocysts during palynological analyses, in particular during stratigraphic studies, resulting in a loss of information. However, significant progress in their taxonomy has been made over the last two decades, and their stratigraphic and paleoenvironmental value is progressively explored. The fossil acritarch genera *Cymatiosphaera* and *Lavradosphaera* have been frequently recorded in the Neogene of the high northern latitudes and exhibit high relative abundances in certain intervals where they may even outnumber the dinocysts (de Vernal and Mudie, 1989; Piasecki, 2003; De Schepper and Head, 2014; Schreck et al., 2013). Despite providing valuable biostratigraphic marker events (Matthiessen et al., 2009; De Schepper and Head, 2014; Mattingsdal et al., 2014; Grøsfjeld et al., 2014), the application of these high abundance intervals (acmes) for paleoenvironmental reconstructions is still restricted due to limited knowledge on their paleoecological implications. At ODP Site 907, acritarchs occur throughout most of the analysed interval and contribute substantially to the palynomorph assemblage (Figs. 2–3). Unfortunately, the Middle Miocene assemblage is dominated by various spinous forms that could not be assigned to a particular genus but have only collectively been referred to as acanthomorphic acritarchs (Schreck et al., 2013), and are hence not discussed here.

Lavradosphaera elongata is restricted to the Middle Miocene in ODP Site 907 and its highest occurrence in the upper Serravallian (Figs. 2–3) has been related to the global Mi-5 cooling event leading to the interpretation of *L. elongata* being a warm-temperate species (Schreck and Matthiessen, 2014). Indeed, its occurrence is confined to SSTs higher than 20 °C (Figs. 8–9) indicating a warm water preference. It exhibits a restricted temperature range between 20 and 24 °C suggesting an adaptation to warmer surface waters, which likely explains its disappearance during times of high latitude cooling. However, this species has only been recorded in the Iceland Sea to date and relative abundances are usually low, thus conclusions should be regarded tentative until more data on its distribution are available to validate the temperature range given in this study.

The acritarch *Decahedrella martinheadii* is endemic to the high northern latitudes and an excellent stratigraphic marker for the Late Miocene in the Arctic and sub-arctic seas (Schreck et al., 2012). Based on its biogeographic distribution it has been considered a cold-water species (Manum, 1997; Matthiessen et al., 2009). Indeed, its first occurrence in Iceland Sea ODP Hole 907A around 10.5 Ma is

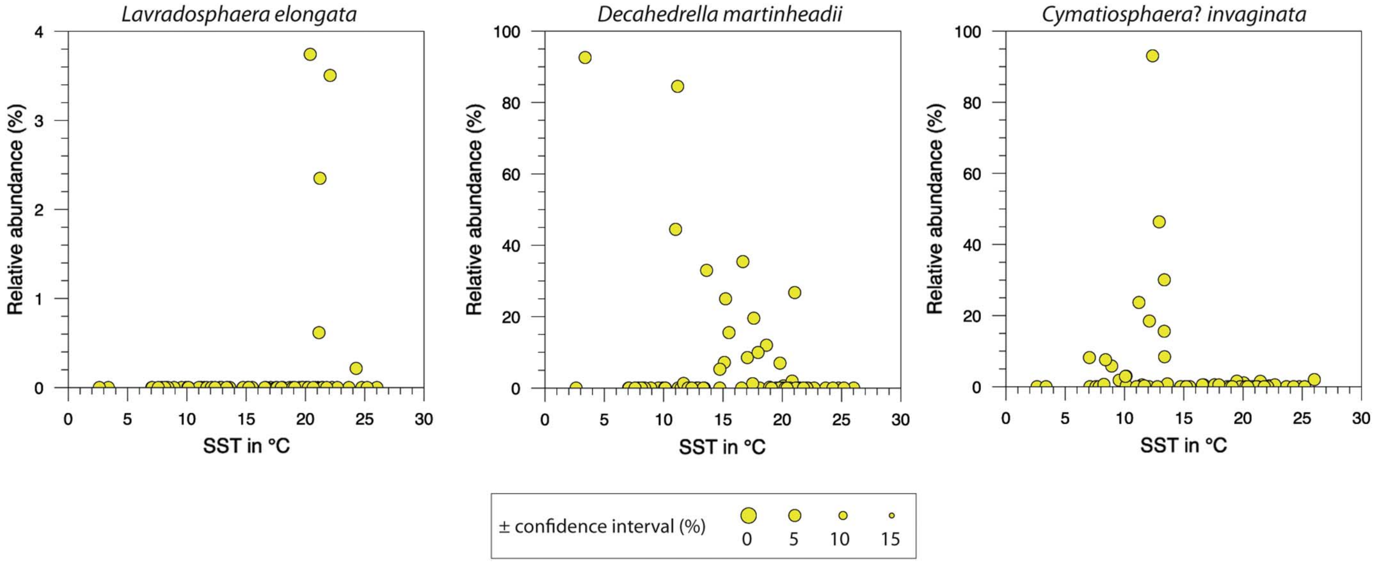

Fig. 8. Relative abundance (in %) of extinct acritarchs in relation to sea-surface temperatures (SST in °C). Species relative abundance (yellow dots) is plotted against alkenone-based SST. (For interpretation of the references to colour in this figure legend, the reader is referred to the web version of this article.)

contemporaneous with the occurrence of the first drop stone, the onset of predominantly siliciclastic deposition at the site (Figs. 2–3, Shipboard Scientific Party, 1995) and a permanent drop of SSTs below 20 °C. In combination with simultaneously declining dinocyst diversity and the disappearance of several dinocyst and acritarch taxa, this suggests initiation of cooler surface water conditions in the study area at that time (Schreck et al., 2013). However, alkenone data from ODP Hole 907A indicate a broad temperature tolerance for this species as it occurs at SSTs ranging from 3 to 21 °C (Figs. 8–9). Although its presence in significant numbers up to 21 °C contrasts previous interpretations of this species being a cold-water indicator based on biogeographic distribution, highest relative abundances of > 40% of the total marine palynomorph assemblage (dinocysts and acritarchs) are found ≤ 12 °C. In the central Arctic Ocean, *D. martinheadii* continuously occurs in samples with alkenone SST estimates ranging from 4 to 6 °C (Stein et al., 2016), which indicates that, even though this species can tolerate a wide range of temperatures, it is well adapted to colder conditions in the Arctic and subarctic realm.

The genus *Cymatiosphaera* has been assigned to the prasinophytes, which today forms an important element of high latitude phytoplankton communities (Tyson, 1995, and references therein). In modern and Quaternary sediments, prasinophytes (in particular *Cymatiosphaera* species) are often associated with cooler surface waters and/or less saline conditions (Wall and Dale, 1974; Tappan, 1980; Sorrel et al., 2006). In the Pliocene of Iceland Sea ODP Hole 907A, *Cymatiosphaera*? *invaginata* reaches relative abundances > 5% of the total marine palynomorph assemblage at temperatures lower than 15 °C (Fig. 8), indeed indicating a cold-water tolerance of this species. The Early Pliocene interval with elevated *C.*? *invaginata* abundance is characterized by severe cooling (Figs. 2–3, De Schepper et al., 2015) and increased occurrence of ice-rafted debris (Fronval and Jansen, 1996), both supporting this interpretation. In the generally warmer Middle Miocene, however, it can occur at temperatures of up to 26 °C, but then never exceeds > 2% of the total marine palynomorph assemblage suggesting an occurrence close to its upper temperature limit. This species apparently tolerates a broad range of temperatures, but relative abundances in ODP Hole 907A clearly suggest an affinity for cooler surface waters.

4. Conclusion

The combination of dinocyst and acritarch assemblages with independently derived alkenone-based SST estimates from the same sample presented here provide an initial quantitative assessment of temperature preferences for Miocene through Pliocene species in a high latitude setting. We refrain from defining exact upper and lower temperature limits for the occurrence of extinct species, but provide temperature ranges in which extinct species may have occurred based on independently derived SST estimates, thus improving previous qualitative assignments that were solely based on biogeographic distribution. Our results indicate that:

- The Miocene dinocyst species *Cerebrocysta irregulare*, *Cordosphaeridium minimum*, *Operculodinium centrocarpum* s.s., *Impagidinium elongatum*, *Batiacasphaera hirsuta* and *Labyrinthodinium truncatum*, and the acritarch *Lavradosphaera elongata* are restricted to a narrow temperature interval and none of these are recorded at SSTs below 15 °C. Therefore, these species are considered as warm-water species. Their disappearance during late Neogene cooling, indicated by a SST decrease and the first drop stone at Site 907, suggests a strong adaptation to the warmer conditions prevailing during most of the Miocene.
- The stratigraphically higher ranging species *Operculodinium*? *eirikianum*, *Reticulatosphaera actinocoronata*, *Batiacasphaera micropapillata* complex and *Habibacysta tectata* tolerate a broader temperature range. The latter two taxa still contribute to the palynomorph assemblage at temperatures below 10 °C, but our data indicate that *H. tectata* is not a cold-water species as previously suggested based on (paleo)biogeographic distribution. In contrast, *B. micropapillata* complex may have a preference for warmer surface conditions than previously suggested by biogeography. *Operculodinium*? *eirikianum* is considered a cold-intolerant species that may have a lower SST limit for its occurrence at around 10 °C.
- The acritarchs *D. martinheadii* and *C.*? *invaginata* have a broad temperature distribution across the Miocene to Pliocene, but high relative abundances at temperatures < 10 °C in the Iceland Sea clearly suggest a preference for cooler surface water conditions. Based on our data quantitative data, however, *D. martinheadii* should not be regarded as an indicator for cold waters exclusively.
- The Miocene-Pliocene distribution of the extant L. *machaerophorum*, *N. labyrinthus*, *A. choane* and *S. elongatus* compares well with its occurrence in the Plio-Pleistocene North Atlantic and in the modern ocean. However, it rather corresponds to the warm end of its distribution in the modern ocean for *S. elongatus* s.l. and *N. labyrinthus*.
- Compared to present-day, the extant *I. pallidum* does not exhibit

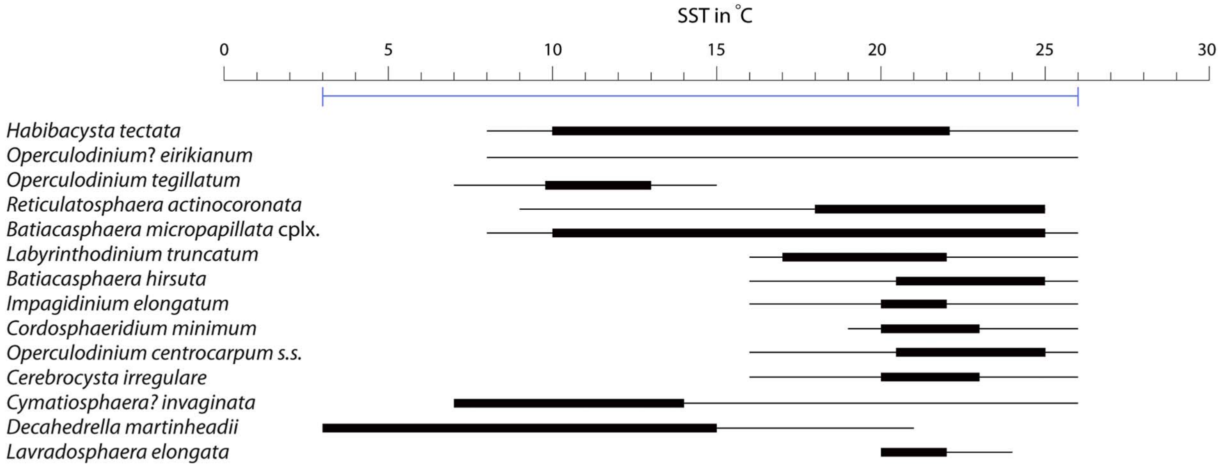

Fig. 9. Summary of the temperature ranges of the extinct dinoflagellate and acritarch species discussed in the text. Highlighted area (black thick line) represents the centre of distribution. Blue line indicates the total reconstructed temperature range in ODP Site 907. (For interpretation of the references to colour in this figure legend, the reader is referred to the web version of this article.)

increased relative abundances at the lower end of its temperature range in both paleo-datasets, but rather show a preference for somewhat warmer waters (> 10 °C) in the geological past. We thus question its use as a reliable cold-water indicator in pre-Quaternary sediments.

Although our Miocene to Pliocene record may be slightly biased towards warmer SSTs when compared to the present-day reference database, fossil and modern distribution of extant species is largely comparable. It is in good agreement with the species distribution recorded in the North Atlantic Plio-Pleistocene paleo-dataset (De Schepper et al., 2011) and therefore provides first indications on how to interpret Miocene assemblages with no modern analogue. In particular, when combining the SST range of several individual species it allows to narrow the interval of co-occurrence and thus to infer the prevailing SSTs at the study site (Fig. 9). Our new data complement the previously published paleo-dataset from the North Atlantic and expands its spatial (high northern latitudes) and temporal (into the Miocene) coverage. However, we note that our data represent an initial assignment of paleoecological affinities of extinct Mio-Pliocene species and there is a strong need to further augment data from different sites to this dataset in order to confirm the proposed relationships and to further increase the reliability of ecological assessments of extinct species.

Despite its limitations, this approach helps to decipher the paleoecology of extinct species and improves their application for paleoenvironmental reconstructions, in particular in the high northern latitudes where other microfossil groups are rare to absent. A refined understanding of temperature preferences of Neogene high latitude species and its quantitative assessment will be particularly important to better understand paleoenvironmental changes in the Arctic Ocean and marginal seas during Earth's transition from Greenhouse to Icehouse conditions.

Acknowledgments

This research uses samples and data provided by the Ocean Drilling Program. We gratefully thank W. Luttmer (AWI-Bremerhaven) for technical support with the alkenone analyses and M. Jones (Palynological Laboratory Services Ltd., Holyhead, UK) for palynological preparation. MS and JM acknowledge financial support from the German Research Foundation (DFG MA 3913/2), and MS is additionally thankful to the Basic Research Program (No. PE16062) of the Korea Polar Research Institute, and a National Research Foundation of Korea grant from the Government of Korea (MSIT) (NRF-2015M1A5A1037243). SDS and CC acknowledge funding from the Norwegian Research Council (project 229819).

Appendix A. List of taxa discussed in the text and their full authorial citations

Ataxiodinium choane Reid, 1974
Batiacasphaera hirsuta Stover, 1977
Batiacasphaera micropapillata Stover, 1977
Cerebrocysta irregulare Schreck et al., 2012
Cordosphaeridium minimum (Morgenroth, 1966) Benedek, 1972
Habibacysta tectata Head et al., 1989
Impagidinium elongatum Schreck et al., 2012
Impagidinium pallidum Bujak, 1984
Labyrinthodinium truncatum Piasecki, 1980
Lingulodinium machaerophorum (Deflandre and Cookson, 1955) Wall, 1967
Nematosphaeropsis labyrinthus (Ostenfeld, 1903) Reid, 1974
Operculodinium centrocarpum (Deflandre and Cookson, 1955) Wall, 1967
Operculodinium tegillatum Head, 1997
Operculodinium? eirikianum Head et al., 1989 emend. Head, 1997
Reticulatosphaera actinocoronata (Benedek, 1972) Bujak and Matsuoka, 1986 emend. Bujak and Matsuoka, 1986
Spiniferites elongatus Reid, 1974
Cymatiosphaera? invaginata Head et al., 1989
Decahedrella martinheadii Manum, 1997
Lavradosphaera elongata Schreck and Matthiessen, 2014

References

Andruleit, H., 1997. Coccolithophore fluxes in the Norwegian-Greenland Sea: seasonality and assemblage alterations. Mar. Micropaleontol. 31, 45–64.
Blindheim, J., Østerhus, S., 2005. The Nordic Seas, main oceanographic features. In: Drange, H., Dokken, T., Furevik, T., Gerdes, R. (Eds.), The Nordic Seas — An Integrated Perspective. American Geophysical Union, Washington D.C., pp. 11–38.
Brenner, W., Biebow, N., 2001. Missing autofluorescence of recent and fossil dinoflagellate cysts — an indicator of heterotrophy? Neues Jb. Geol. Paläntol. Abh. 219, 229–240.
Bujak, J.P., 1984. Cenozoic dinoflagellate cysts and acritarchs from the Bering Sea and northern North Pacific, DSDP Leg 19. Micropaleontology 30, 180–212.
Channell, J.E.T., Amigo, A.E., Fronval, T., Rack, F., Lehman, B., 1999. Magnetic stratigraphy at Sites 907 and 985 in the Norwegian-Greenland Sea and a revision of the Site 907 composite section. In: Raymo, M.E., Jansen, E., Blum, P., Herbert, T.D. (Eds.), Proceedings of the Ocean Drilling Program, Scientific Results 162. College Station, TX, pp. 131–148.
Chapman, M., 2010. Seasonal production patterns of planktonic foraminifera in the NE Atlantic Ocean: implications for paleotemperature and hydrographic reconstructions. Paleoceanography 25, PA1101. http://dx.doi.org/10.1029/2008PA001708.

Dale, B., 1996. Dinoflagellate cyst ecology: modelling and geological applications. In: Jansonius, J., McGregor, D.C. (Eds.), Palynology: Principles and Applications, Vol. 3. AASP Foundation, Dallas, TX, pp. 1249–1275.

Dale, A.L., Dale, B., 1992. Dinoflagellate contributions to the sediment flux of the Nordic Sea. In: Honjo, S. (Ed.), Dinoflagellate Contribution to the Deep Sea. Ocean Biocoenosis Series No. 5 Woods Hole Oceanographic Institution, Massachusetts, pp. 45–75.

De Schepper, S., Head, M.J., 2008. New dinoflagellate cyst and acritarch taxa from the Pliocene and Pleistocene of the eastern North Atlantic (DSDP Site 610A). J. Syst. Palaeontol. 6, 101–107.

De Schepper, S., Head, M.J., 2014. New Pliocene and Pleistocene acritarchs: correlation potential in high latitude oceans. J. Syst. Palaeontol. 12, 493–519.

De Schepper, S., Fischer, E.I., Groeneveld, J., Head, M.J., Matthiessen, J., 2011. Deciphering the palaeoecology of Late Pliocene and Early Pleistocene dinoflagellate cysts. Palaeogeogr. Palaeoclimatol. Palaeoecol. 309, 17–32.

De Schepper, S., Schreck, M., Beck, K.M., Matthiessen, J., Fahl, K., Mangerud, G., 2015. Early Pliocene onset of modern Nordic Seas circulation related to ocean gateway changes. Nat. Commun. 6. http://dx.doi.org/10.1038/ncomms9659.

De Schepper, S., Beck, K.M., Mangerud, G., 2017. Late Neogene dinoflagellate cyst and acritarch biostratigraphy for Ocean Drilling Program Hole 642B, Norwegian Sea. Rev. Palaeobot. Palynol. 236, 12–32.

Edwards, L.E., Mudie, P.J., de Vernal, A., 1991. Pliocene paleoclimatic reconstruction using dinoflagellate cysts: comparison of methods. Quat. Sci. Rev. 10, 259–274.

Elderfield, H., Ganssen, G., 2000. Past temperature and δ^{18}O of surface ocean waters inferred from foraminiferal Mg/Ca ratios. Nature 405, 442–445.

Fronval, T., Jansen, E., 1996. Late Neogene paleoclimates and paleoceanography in the Iceland-Norwegian Sea: evidence from the Iceland and Vøring Plateaus. In: Thiede, J., Myhre, A.M., Firth, J.V., Johnson, G.L., Ruddiman, W.F. (Eds.), Proceedings of the Ocean Drilling Program, Scientific Results 151. College Station, TX, pp. 455–468.

Ganssen, G.M., Kroon, D., 2000. The isotopic signature of planktonic foraminifera from NE Atlantic surface sediments: implications for the reconstruction of past oceanic conditions. J. Geol. Soc. 157, 693–699.

Grøsfjeld, K., De Schepper, S., Fabian, K., Husum, K., Baranwal, S., Andreassen, K., Knies, J., 2014. Dating and palaeoenvironmental reconstruction of the sediments around the Miocene/Pliocene boundary in Yermak Plateau ODP Hole 911A using marine palynology. Palaeogeogr. Palaeoclimatol. Palaeoecol. 414, 382–402.

Guiot, J., de Vernal, A., 2007. Transfer functions: methods for quantitative paleoceanography based on microfossils. In: Hillaire-Marcel, C., de Vernal, A. (Eds.), Proxies in Late Cenozoic Paleoceanography. Elsevier, Amsterdam, pp. 523–563.

Head, M.J., 1994. Morphology and paleoenvironmental significance of the Cenozoic dinoflagellate genera *Tectatodinium* and *Habibacysta*. Micropaleontology 40, 289–321.

Head, M.J., 1997. Thermophilic dinoflagellate assemblages from the mid Pliocene of eastern England. J. Paleontol. 71, 165–193.

Head, M.J., Norris, G., 1989. Palynology and dinocyst stratigraphy of the Eocene and Oligocene in ODP Leg 105, Hole 647A, Labrador Sea. In: Srivastava, S.P., Arthur, M., Clement, B. (Eds.), Proceedings of the Ocean Drilling Program, Scientific Results 105. College Station, TX, pp. 515–550.

Heikkilä, M., Pospelova, V., Forest, A., Stern, G.A., Fortier, L., Macdonald, R.W., 2016. Dinoflagellate cyst production over an annual cycle in seasonally ice-covered Hudson Bay. Mar. Micropaleontol. 125, 1–24.

Hennissen, J.A., Head, M.J., De Schepper, S., Groeneveld, J., 2017. Dinoflagellate cyts paleoecology during the Pliocene-Pleistocene transition in the North Atlantic. Palaeogeogr. Palaeoclimatol. Palaeoecol. 470, 81–108.

Herbert, T., 2003. Alkenone paleotemperature determinations. In: Holland, H.D., Turekian, K.K. (Eds.), Treatise of Geochemistry — Volume 6: The Oceans and Marine Geochemistry. Elsevier, Amsterdam, pp. 391–432.

Herbert, T., Lawrence, K.T., Tzanova, A., Peterson, L.C., Caballero-Gill, R., Kelly, C.S., 2016. Late Miocene global cooling and the rise of modern ecosystems. Nat. Geosci. 9, 843–847.

Hilgen, F.J., Lourens, L.J., Van Dam, J.A., 2012. The Neogene period. In: Gradstein, F., Ogg, J., Schmitz, M., Ogg, G. (Eds.), The Geological Time Scale 2012. Elsevier, Amsterdam, pp. 923–978.

Howe, J.A., Harland, R., Cottier, F.R., Brand, T., Willis, K.J., Berge, J.R., Grøsfjeld, K., Eriksson, A., 2010. Dinoflagellate cysts as proxies for palaeoceanographic conditions in Arctic fjords. In: Howe, J.A., Austin, W.E.N., Forwick, M., Paetzel, M. (Eds.), Fjord Systems and Archives. Geological Society of London, London, pp. 61–74.

Jiménez-Moreno, G., Head, M.J., Harzhauser, M., 2006. Early and Middle Miocene dinoflagellate cyst stratigraphy of the Central Paratethys, Central Europe. J. Micropalaeontol. 25, 113–119.

Lourens, L., Hilgen, F., Shackleton, N.J., Laskar, J., Wilson, J., 2005. The Neogene. In: Gradstein, F.M., Ogg, J.G., Smith, A.G. (Eds.), A Geological Timescale 2004. Cambridge University Press, Cambridge, U.K., pp. 409–430.

Louwye, S., 2002. Dinoflagellate cyst biostratigraphy of the Upper Miocene Deurne Sands (Diest Formation) of northern Belgium, southern North Sea Basin. Geol. J. 37, 55–67.

Louwye, S., De Schepper, S., 2010. The Miocene–Pliocene hiatus in the southern North Sea Basin (northern Belgium) revealed by dinoflagellate cysts. Geol. Mag. 147, 1–17.

Louwye, S., Foubert, A., Mertens, K., Van Rooij, D., IODP Expedition 307 Scientific Party, 2007. Integrated stratigraphy and palaeoecology of the Lower and Middle Miocene of the Porcupine Basin. Geol. Mag. 145, 321–344.

Manum, S.B., 1997. *Decahedrella martinheadii* gen. et sp. nov. — a problematic palynomorph from the Northern Atlantic Miocene. Palynology 21, 67–77.

Marret, F., Eirìksson, J., Knudsen, K.L., Turon, J.-L., Scourse, J.D., 2004. Distribution of dinoflagellate cyst assemblages in surface sediments from the northern and western shelf of Iceland. Rev. Palaeobot. Palynol. 128, 35–53.

Masure, E., Vrielynck, B., 2009. Late Albian dinoflagellate cyst paleobiogeography as indicator of asymmetric sea surface temperature gradient on both hemispheres with southern high latitudes warmer than northern ones. Mar. Micropaleontol. 70, 120–133.

Matthiessen, J., 1995. Distribution patterns of dinoflagellate cysts and other organic-walled microfossils in recent Norwegian-Greenland Sea sediments. Mar. Micropaleontol. 24, 307–334.

Matthiessen, J., De Vernal, A., Head, M.J., Okolodkov, Y., Puerto, A., Zonneveld, K.A.F., Harland, R., 2005. Modern organic-walled dinoflagellate cysts in Arctic marine environments and their (paleo-) environmental significance. Paläontol. Z. 79, 3–51.

Matthiessen, J., Brinkhuis, H., Poulsen, N.E., Smelror, M., 2009. *Decahedrella martinheadii* Manum 1997 — a stratigraphically and paleoenvironmentally useful Miocene acritarch of the northern high latitudes. Micropaleontology 55, 171–186.

Mattingsdal, R., Knies, J., Andreassen, K., Fabian, K., Husum, K., Grøsfjeld, K., De Schepper, S., 2014. A new 6 Myr stratigraphic framework for the Atlantic–Arctic Gateway. Quat. Sci. Rev. 92, 170–178.

Mollenhauer, G., Kienast, M., Lamy, F., Meggers, H., Schneider, R.R., Hayes, J.M., Eglinton, T.I., 2005. An evaluation of ^{14}C age relationships between co-occurring foraminifera, alkenones, and total organic carbon in continental margin sediments. Paleoceanography 20, PA1016. http://dx.doi.org/10.1029/2004PA001103.

Müller, P.J., Kirst, G., Ruhland, G., von Storch, I., Rosell-Melé, A., 1998. Calibration of the alkenone paleotemperature index $U^{k'}_{37}$ based on core-tops from the eastern South Atlantic and the global ocean (60°N-60°S). Geochim. Cosmochim. Acta 62, 1757–1772.

Shipboard Scientific Party, 1995. Site 907. In: Myhre, A.M., Thiede, J., Firth, J.V. (Eds.), Proceedings of the Ocean Drilling, Initial Reports 151. College Station, TX, pp. 57–111.

Piasecki, S., 2003. Neogene dinoflagellate cysts from Davis Strait, offshore West Greenland. Mar. Pet. Geol. 20, 1075–1088.

Quaijtaal, W., Donders, T.H., Persico, D., Louwye, S., 2014. Characterising the middle Miocene Mi-events in the Eastern North Atlantic realm: A first high-resolution marine palynological record from the Porcupine Basin. Palaeogeogr. Palaeoclimatol. Palaeoecol. 399, 140–159.

Radi, T., de Vernal, A., 2008. Dinocysts as proxy of primary productivity in mid-high latitudes of the Northern Hemisphere. Mar. Micropaleontol. 68, 84–114.

Rosell-Melè, A., McClymont, E., 2007. Biomarkers as paleoceanographic proxies. In: Hillaire-Marcel, C., de Vernal, A. (Eds.), Proxies in Late Cenozoic Paleoceanography. Elsevier, Amsterdam, pp. 441–490.

Samtleben, C., Bickert, T., 1990. Coccoliths in sediment traps from the Norwegian Sea. Mar. Micropaleontol. 16, 39–64.

Samtleben, C., Schäfer, P., Andruleit, H., Baumann, A., Baumann, K.H., Kohly, A., Matthiessen, J., Schröder-Ritzrau, A., 1995. Plankton in the Norwegian-Greenland Sea: from living communities to sediment assemblages — an actualistic approach. Geol. Rundsch. 84, 108–136.

Schreck, M., Matthiessen, J., 2013. *Batiacasphaera micropapillata*: palaeobiogeographic distribution and palaecological implications of a critical Neogene species complex. In: Lewis, J., Marret, F., Bradley, L. (Eds.), Biological and Geological Perspectives of Dinoflagellates. The Micropalaeontological Society, Special Publications Geological Society, London, pp. 301–314.

Schreck, M., Matthiessen, J., 2014. *Batiacasphaera bergenensis* and *Lavradosphaera elongata* — new dinoflagellate cyst and acritarch species from the Miocene of the Iceland Sea (ODP Hole 907A). Rev. Palaeobot. Palynol. 211, 97–106.

Schreck, M., Matthiessen, J., Head, M.J., 2012. A magnetostratigraphic calibration of Middle Miocene through Pliocene dinoflagellate cyst and acritarch events in the Iceland Sea (Ocean Drilling Program Hole 907A). Rev. Palaeobot. Palynol. 187, 66–94.

Schreck, M., Meheust, M., Stein, R., Matthiessen, J., 2013. Response of marine palynomorphs to Neogene climate cooling in the Iceland Sea (ODP Hole 907A). Mar. Micropaleontol. 101, 49–67.

Schröder-Ritzrau, A., Andruleit, H., Jensen, S., Samtleben, C., Schäfer, P., Matthiessen, J., Hass, C., Kohly, A., Thiede, J., 2001. Distribution, export and alteration of fossilizable plankton in the Nordic seas. In: Schäfer, P., Ritzrau, W., Schlüter, M., Thiede, J. (Eds.), The Northern North Atlantic — A Changing Environment. Springer-Verlag, Berlin, pp. 81–104.

Sison, C.P., Glaz, J., 1995. Simultaneous confidence intervals and sample size determination for multinomial proportions. J. Am. Stat. Assoc. 90, 366–369.

Sorrel, P., Popescu, S.M., Head, M.J., Suc, J.P., Klotz, S., Oberhänsli, H., 2006. Hydrographic development of the Aral Sea during the last 2000 years based on a quantitative analysis of dinoflagellate cysts. Palaeogeogr. Palaeoclimatol. Palaeoecol. 234, 304–327.

Stabell, B., Koç, N., 1996. Recent to Middle Miocene diatom productivity at Site 907, Iceland Plateau. In: Thiede, J., Myhre, A.M., Firth, J.V., Johnson, G.L., Ruddiman, W.F. (Eds.), Proceedings of the Ocean Drilling Program, Scientific Results 151. College Station, TX, pp. 483–492.

Stein, R., Fahl, K., Schreck, M., Knorr, G., Niessen, F., Jensen, L., Forwick, M., Gebhardt, C., Kaminski, M., Kopf, A., Matthiessen, J., Jokat, W., Lohmann, G., 2016. Evidence for ice-free summers in the late Miocene central Arctic Ocean. Nat. Commun. 7. http://dx.doi.org/10.1038/ncomms11148.

Stephens, C., Conkright, M.E., Boyer, T.P., Antonov, J.I., Baranova, O.K., Garcia, H.E., Gelfeld, R., Johnson, D., Locarnini, R.A., Murphy, P.P., O'Brien, T.D., Smolyar, I., 2002. In: Levitus, S. (Ed.), World Ocean Database 2001, Volume 3: Temporal Distribution of Conductivity–Temperature–Depth (Pressure) Profiles. NOAA Atlas NESDIS 44 U.S. Government Printing Office, Washington, D.C. (47 pp).

Stockmarr, J., 1977. Tablets with spores used in absolute pollen analysis. Pollen Spores 13, 615–621.

Tappan, H., 1980. The Paleobiology of Plant Protists. W.H. Freeman and Company, San Francisco (1028 pp).

Taylor, F.J.R., 1987. The Biology of Dinoflagellates. Blackwell Scientific Publications, Oxford (785 pp).

Tyson, R.V., 1995. Sedimentary Organic Matter — Organic Facies and Palynofacies. Chapman & Hall, London (615 pp).

Van Nieuwenhove, N., Baumann, A., Matthiessen, J., Bonnet, S., de Vernal, A., 2016. Sea surface conditions in the southern Nordic Seas during the Holocene based on dinoflagellate cyst assemblages. The Holocene 26, 722–735.

Vázquez-Riveiros, N., Govin, A., Waelbroeck, C., Mackensen, A., Michel, E., Moreira, S., Bouinot, T., Caillon, N., Orgun, A., Brandon, M., 2016. Mg/Ca thermometry in planktic foraminifera: Improving paleotemperature estimations for *G. bulloides* and *N. pachyderma* left. Geochem. Geophys. Geosyst. 17, 1–16.

de Vernal, A., Mudie, P., 1989. Pliocene and Pleistocene palynostratigraphy at ODP Sites 646 and 647, eastern and southern Labrador Sea. In: Srivastava, S.P., Arthur, M., Clement, B. (Eds.), Proceedings of the Ocean Drilling Program, Scientific Results 105. College Station, TX, pp. 401–422.

de Vernal, A., Henry, J., Matthiessen, J., Mudie, P., Rochon, A., Boessenkool, K.P., Eynaud, F., Grosfjeld, K., Guiot, J., Hamel, D., Harland, R., Head, M.J., Kunz-Pirrung, M., Levac, E., Loucheur, V., Peyron, O., Pospelova, V., Radi, T., Turon, J.L., Voronina, E., 2001. Dinoflagellate cyst assemblages as tracers of sea-surface conditions in the northern North Atlantic, Arctic, and sub-Arctic seas: the new “n = 677” data base and its application for quantitative paleoceanographic reconstruction. J. Quat. Sci. 16, 681–698.

de Vernal, A., Eynaud, F., Henry, M., Hillaire-Marcel, C., Londeix, L., Mangin, S., Matthiessen, J., Marret, F., Radi, T., Rochon, A., Solignac, S., Turon, J.L., 2005. Reconstruction of sea-surface conditions at middle to high latitudes of the Northern Hemisphere during the Last Glacial Maximum (LGM) based on dinoflagellate cyst assemblages. Quat. Sci. Rev. 24, 897–924.

de Vernal, A., Rochon, A., Fréchette, B., Henry, M., Radi, T., Solignac, S., 2013. Reconstructing past sea ice cover of the Northern Hemisphere from dinocyst assemblages: status of the approach. Quat. Sci. Rev. 79, 122–134.

Versteegh, G.J.M., 1994. Recognition of cyclic and non-cyclic environmental changes in the Mediterranean Pliocene: a palynological approach. Mar. Micropaleontol. 23, 147–183.

Versteegh, G.J.M., Zonneveld, K.A.F., 1994. Determination of (palaeo-)ecological preferences of dinoflagellates by applying Detrended and Canonical Correspondence analysis to Late Pliocene dinoflagellate cyst assemblages of the south Italian Singa section. Rev. Palaeobot. Palynol. 84, 181–199.

Wall, D., Dale, B., 1974. Dinoflagellates in the Late Quaternary deep-water sediments of the Black Sea. In: Degens, E.T., Ross, D.A. (Eds.), The Black Sea — Geology, Chemistry and Biology. American Association of Petroleum Geologists, Tulsa, TX, pp. 364–380.

Williams, G.L., Fensome, R.A., MacRae, R.A., 2017. The Lentin and Williams Index of Fossil Dinoflagellates, 2017 edition. American Association of Stratigraphic Palynologists, Contribution Series 48, TX (1097 pp).

Wrenn, J.H., Kokinos, J.P., 1986. Preliminary comments on Miocene through Pleistocene dinoflagellate cysts from De Soto Canyon, Gulf of Mexico. In: American Association of Stratigraphic Palynologists, Contributions Series 17, TX, pp. 169–225.

Zachos, J.C., Dickens, G.R., Zeebe, R.E., 2008. An early Cenozoic perspective on greenhouse warming and carbon-cycle dynamics. Nature 451, 279–283.

Zonneveld, K.A.F., Versteegh, G., Kodrans-Nsiah, M., 2008. Preservation and organic chemistry of Late Cenozoic organic-walled dinoflagellate cysts: a review. Mar. Micropaleontol. 68, 179–197.

Zonneveld, K.A.F., Marret, F., Versteegh, G.J.M., Bogus, K., Bonnet, S., Bouimetarhan, I., Crouch, E., de Vernal, A., Elshanawany, R., Edwards, L., Esper, O., Forke, S., Grøsfjeld, K., Henry, M., Holzwarth, U., Kielt, J.-F., Kim, S.-Y., Ladouceur, S., Ledu, D., Chen, L., Limoges, A., Londeix, L., Lu, S.H., Mahmoud, M.S., Marino, G., Matsouka, K., Matthiessen, J., Mildenhal, D.C., Mudie, P., Neil, H.L., Pospelova, V., Qi, Y., Radi, T., Richerol, T., Rochon, A., Sangiorgi, F., Solignac, S., Turon, J.-L., Verleye, T., Wang, Y., Wang, Z., Young, M., 2013. Atlas of modern dinoflagellate cyst distribution based on 2405 data points. Rev. Palaeobot. Palynol. 191, 1–197.